IEEE Transactions on Signal Processing

Analysis and Realization of Amplitude Sampling

Journal:	*Transactions on Signal Processing*
Manuscript ID	T-SP-22230-2017
Manuscript Type:	Regular Paper
Date Submitted by the Author:	31-May-2017
Complete List of Authors:	Martínez-Nuevo, Pablo; Massachusetts Institute of Technology, Electrical Engineering and Computer Science; Bang og Olufsen, R&D Acoustics Lai, Hsin-Yu; Massachusetts Institute of Technology, Electrical Engineering and Computer Science Oppenheim, Alan V.; Massachusetts Institute of Technology, Research Laboratory of Electronics
EDICS:	28. DSP-SAMP Sampling, extrapolation, and interpolation < DSP DIGITAL AND MULTIRATE SIGNAL PROCESSING, 29. DSP-TFSR Time-frequency analysis and signal representation < DSP DIGITAL AND MULTIRATE SIGNAL PROCESSING, 24. DSP-CPSL Compressive and nonuniform sampling < DSP DIGITAL AND MULTIRATE SIGNAL PROCESSING, 30. DSP-TRSF Transforms for signal processing < DSP DIGITAL AND MULTIRATE SIGNAL PROCESSING, 21. DSP-ALGO Algorithm analysis < DSP DIGITAL AND MULTIRATE SIGNAL PROCESSING

Analysis and Realization of Amplitude Sampling

Pablo Martínez-Nuevo, Hsin-Yu Lai, *Student Member, IEEE,* and Alan V. Oppenheim, *Life Fellow, IEEE*

***Abstract*—The theoretical basis for conventional acquisition of bandlimited signals typically relies on uniform time sampling and assumes infinite-precision amplitude values. In this paper, we explore signal representation and recovery based on uniform amplitude sampling with assumed infinite precision timing information. The approach is based on the concept of reversibly transforming a nonmonotonic input signal into a monotonic one which is then uniformly sampled in amplitude. In effect, the monotonic function is then represented by the times at which the signal crosses a predefined and equally-spaced set of amplitude values. We refer to this technique as amplitude sampling. When the transformation into a monotonic function is based on ramp addition, for practical purposes, the approach can be implemented by applying a one-level level-crossing detector to the result of adding an appropriate sawtooth-like waveform to the source signal. The time sequence generated by the level crossings can be interpreted alternatively as nonuniform time sampling of the original source signal or uniform amplitude sampling of the monotonic function to which it is transformed. We derive duality and frequency-domain properties for the functions involved in the transformation. Iterative algorithms are proposed and implemented for recovery of the original source signal and compared with nonuniform time sampling reconstruction methods of the original source signal. As indicated in the simulations, the proposed iterative amplitude-sampling algorithm achieves a faster convergence rate than reconstruction based on nonuniform sampling. The performance can also be improved by appropriate choice of the parameters while maintaining the same sampling density.**

***Index Terms*—Sampling theory, level-crossing sampling, nonuniform sampling and reconstruction, iterative algorithms.**

I. Introduction

THE theoretical foundation of conventional time sampling typically relies on the sampling theorem for bandlimited signals [1]–[3], which states that bandlimited signals can be perfectly represented by infinite-precision amplitude values taken at equally-spaced time instants appropriately separated. In this paper, we propose signal representation based on equally-spaced amplitude samples with infinite-precision timing information.

Signal representation based on discrete amplitudes and continuous time has previously been studied and utilized in a number of context. In [4] signal representation consists of the real and complex zeros of a bandlimited signal. Logan's theorem [5] characterizes a subclass of bandpass signals that can be completely represented, up to a scaling factor, by their zero crossings. Practical algorithms for recovery from zero crossings of periodic signals in this class have been proposed in [6]. Arbitrary bandlimited signals can also be implicitly described by the zero crossings of a function resulting from an invertible transformation [7]–[9]—for example, the addition of a sinewave [10, Theorem 1]. In principle, interpolation is possible through Hadamard's factorization [11, Chapter 5] although there are more efficient techniques in terms of convergence rate [12]–[15]. Zero-crossings have also been studied in relation to wavelet transforms [16]. In this case, stable reconstruction can be achieved by including additional information about the original signal.

The extension from zero crossings to multiple levels, in the context of data compression, was investigated in [17]. In that work, a sample is generated whenever the source signal crosses a predefined set of threshold levels. The time instants of the crossings and the level-crossings directions were utilized to represent the signal although time was still quantized due to practical considerations. A practical continuous-time version of level-crossing sampling was later proposed in [18]. Asynchronous delta modulation [19] is, also, in some sense, a precursor of level-crossing sampling since it generates a positive or negative pulse at time instants when the change in signal amplitude surpasses a fixed quantity.

The focus of previous work on level-crossing sampling and reconstruction has typically been approximate reconstruction and implementational simplicity. For example, recovery is often performed through a zero- or first-order hold, possibly in combination with low-pass filtering [20], [21]. Although there exist elaborate reconstruction techniques for multidimensional signals [22], [23], practical and accurate signal reconstruction techniques for generalized level-crossing sampling in one dimension are still under-explored.

In this paper, we explore the concept of amplitude sampling with the signal represented by the time sequence of equally-spaced level crossings. In principle, if a signal were monotonic, then the crossings of equally-spaced amplitude levels would generate an ordered time sequence $\{t_n\}$ which could be considered as a representation of the signal. In effect, under appropriate conditions, this corresponds to uniform sampling in amplitude with the signal information contained in the time sequence $\{t_n\}$. Nonmonotonic signals can be reversibly transformed into monotonic ones which are then uniformly sampled in amplitude. We refer to this technique as amplitude sampling. As discussed in section II, when the reversible transformation consists of adding a ramp with appropriate slope, a more practical implementation to generate the identical ordered time sequence $\{t_n\}$ is that shown in Fig. 1. As shown in II the

This work was supported in part by Texas Instruments Leadership University Program. The work of P. Martínez-Nuevo was also supported in part by Fundación Rafael del Pino, Madrid, Spain. The work of H. Lai was also supported in part by the Jacobs Fellowship and the Siebel Fellowship.

P. Martínez-Nuevo was with the Department of Electrical Engineering and Computer Science, Massachusetts Institute of Technology. He is now with the research department at Bang&Olufsen, 7600 Struer, Denmark (e-mail: pmnuevo@alum.mit.edu).

H. Lai and A. V. Oppenheim are with the Department of Electrical Engineering and Computer Science, Massachusetts Institute of Technology, Cambridge MA 02139 USA (e-mail: hsinyul@mit.edu; avo@mit.edu).

Manuscript received April 19, 2005; revised August 26, 2015.

time sequence generated by the system in Fig. 1 and that obtained by uniform amplitude sampling after ramp addition are identical. For conceptual simplicity in the analysis in this paper, we utilize the interpretation of the time sequence $\{t_n\}$ as derived from uniform amplitude sampling of the monotonic function obtained by ramp addition.

In sections III, IV, and V we derive duality as well as time- and frequency-domain properties relating the functions present in the transformation. The structure of these functions suggest an iterative reconstruction algorithm for numerical recovery of the source signal from the amplitude samples. This algorithm is discussed in Section VI with simulations and comparisons with reconstruction based on the nonuniform time samples.

II. Principle of Amplitude Sampling

Consider first the process represented by the block diagram depicted in Fig. 1. The level detector produces an impulse at times at which the input signal reaches the value Δ. For ease of illustration, assume the ramp-segment generator initiates a ramp with slope $\alpha > 0$ that abruptly shifts down by Δ in amplitude whenever an impulse arrives. Assume α is chosen such that $\tilde{g}(t)$ is monotonic in each interval between successive impulses.

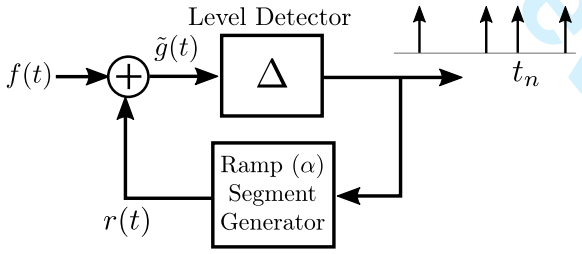

Fig. 1. Equivalent representation of the amplitude sampling process.

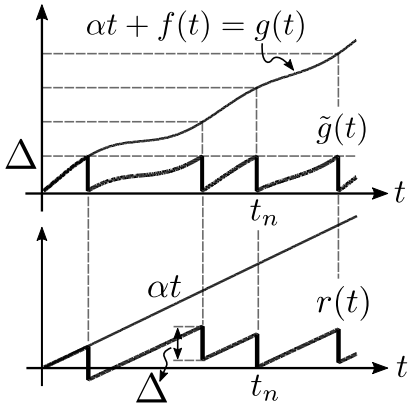

Fig. 2. Illustration of the different waveforms involved in the system shown in Fig. 1.

Fig. 2 shows an example of the signals involved in the process. By construction, the ramp segments of the function $r(t)$ present the same slope. This manifests itself in the presence of an continuous ramp of slope α separated by multiples of Δ for each corresponding segment. Consequently, the function $\tilde{g}(t)$, which is the addition of these segments and the input signal $f(t)$, presents the same characteristic with respect to $g(t) = \alpha t + f(t)$. In fact, the time instants at which the impulses are generated correspond precisely to the level-crossing instants of $g(t)$ for amplitude thresholds placed at multiples of Δ. Moreover, the function $g(t)$, assuming appropriate regularity conditions, has an inverse function $t(g)$ which is effectively sampled uniformly in the amplitude domain with samples corresponding to these time instants. Therefore, the sampling process of Fig. 1 can be interpreted as uniformly sampling the function $t(g)$. In principle, it is possible to generalize this this concept by considering any transformation that generates a monotonic function $g(t)$.

Amplitude sampling and reconstruction as developed in this paper is then based on the principle of reversibly representing and then sampling a time function $g(t)$ in the form $t(g)$ and then sampling in g. This requires that $g(t)$ be monotonic which means that if the source signal is nonmonotonic, it must first be reversibly transformed into a strictly monotonic function through a transformation ϕ. As illustrated in Fig. 3, the resulting function $\phi(f(t))$ is then uniformly sampled. The time instants $\{t_n\}$ at which $\phi(f(t))$ crosses the predefined set of amplitude values $\{n\Delta\}$ implicitly represents the source signal, i.e. $\phi(f(t_n)) = n\Delta$ where $\Delta > 0$ is the separation between consecutive levels. Each of the time instants is paired exactly with one amplitude level. Thus, there exists a one-to-one correspondence between amplitude values and time instants. The sequence of time instants together with knowledge of Δ is sufficient information to describe the sampling process.

Amplitude sampling corresponds to signal-dependent nonuniform time sampling with the sampling density dependent on the source signal and the choice of the transformation ϕ.

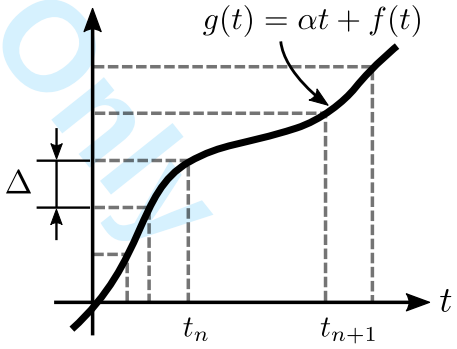

Fig. 3. Principle of amplitude sampling based on a transformation ϕ of the source signal f resulting in a monotonic function $\phi(f(t))$.

III. Transformation by Ramp Addition

There exist a myriad of transformations ϕ that can potentially generate a monotonic function from a given f. Among the simplest is the addition of a ramp with a sufficiently large slope. Suppose the original signal f is continuous, and it is possible to construct the strictly monotonic function $g(t) = \alpha t + f(t)$ for some $\alpha \in \mathbb{R}$. Then, the sampling process consists of the sequence of time instants $\{t_n\}$ satisfying $g(t_n) = \alpha t_n + f(t_n) = n\Delta$ for some $\Delta > 0$.

As indicated earlier, for analysis purposes in this paper, it is convenient to interpret the time sequence $\{t_n\}$ as resulting from sampling uniformly in amplitude the monotonic function $u = g(t) = \alpha t + f(t)$. In the context of this transformation, there exists an inverse function $g^{-1}(u)$ that we choose to express in the form $g^{-1}(u) = u/\alpha + h(u)$ for some amplitude-time function h. This interpretation suggests that this transformation can also be viewed as a mapping from f to the associated function h.

A. Mapping between f and h

The addition of a ramp represents a mapping, parametrized by the slope of the ramp, between the original signal and the function h. We denote this mapping by M_α, i.e. $M_\alpha f = h$ which can be viewed as the addition of the ramp to obtain the monotonic function g and, after inverting g, subtracting the ramp u/α to obtain h. The reverse procedure to recover f from h consists of adding a ramp of slope u/α to h and utilizing the invertibility of g^{-1} as well as the correspondence between g and f. This inverse mapping is denoted by $M_{\alpha^{-1}}$ and satisfies $M_{\alpha^{-1}} h = f$. Fig. 4 illustrates the one-to-one correspondence between f and h. These mappings are also summarized in equation form as [24]

$$\begin{aligned} f(t) &= -\alpha h(f(t) + \alpha t) \\ h(u) &= -\frac{1}{\alpha} f(h(u) + \frac{u}{\alpha}). \end{aligned} \tag{1}$$

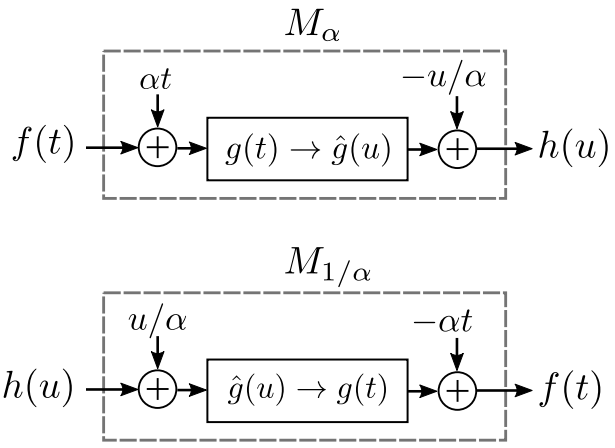

Fig. 4. Illustration of the invertibility of the transformation between f and h when $g(t) = \alpha t + f(t)$ and $g^{-1}(u) = u/\alpha + h(u)$.

As is evident from Fig. 4 and (1) there is a duality between M_α and its inverse. It is possible to interpret (1) as a signal-dependent warping operation that obtains f from h and vice versa. The addition of a ramp in amplitude sampling also generates an underlying mapping, dependent on f or h, between time t and amplitude u. Both mappings can be easily seen from (1) in its matrix form and the corresponding inverse matrix:

$$\begin{pmatrix} f(t) \\ t \end{pmatrix} = \begin{pmatrix} -\alpha & 0 \\ 1 & 1/\alpha \end{pmatrix} \begin{pmatrix} h(u) \\ u \end{pmatrix} \tag{2}$$

$$\begin{pmatrix} h(u) \\ u \end{pmatrix} = \begin{pmatrix} -1/\alpha & 0 \\ 1 & \alpha \end{pmatrix} \begin{pmatrix} f(t) \\ t \end{pmatrix}. \tag{3}$$

The duality implies that any properties of h inherited by assumptions made on f hold for f if the same assumptions are instead imposed on h.

B. The Sampling Process

Amplitude sampling produces a sequence of time instants corresponding to $n\Delta = g(t_n) = \alpha t_n + f(t_n)$ where $\Delta > 0$. In similar fashion, the inverse function $g^{-1}(u)$ and h are both uniformly sampled in amplitude, i.e.

$$g^{-1}(n\Delta) = n\Delta/\alpha + h(n\Delta) \tag{4}$$

and

$$h(n\Delta) = t_n - n\Delta/\alpha. \tag{5}$$

C. Sampling Density

As noted earlier, amplitude sampling in the form presented here can be viewed as equivalent to nonuniform time sampling. In this setting, stable reconstruction algorithms typically impose conditions on the sequence of sampling instants as for example the Landau rate [25] for bandlimited signals. In order to gain insight into the time-sampling density inherent in our amplitude-sampling process, assume the source signal f has a bounded derivative, i.e. $|f'(t)| \leq B$ for some $B > 0$ and that $|\alpha| > B$ so that the function $g(t) = \alpha t + f(t)$ is strictly monotonic. Then the time between successive samples satisfies the inequality

$$\frac{\Delta}{|\alpha| + B} \leq |t_{n+1} - t_n| \leq \frac{\Delta}{|\alpha| - B}. \tag{6}$$

where $\Delta > 0$ is the separation between consecutive amplitude levels.

The bounds in (6) are consistent with intuition. For example, assume that α is positive. The derivative of g is bounded by $\alpha + B$ which provides the minimum attainable time separation between crossings. Similarly, the maximum separation is essentially limited by $\alpha - B$. The quantization step Δ represents the change in amplitude necessary to produce a sample. Additionally, when α achieves sufficiently large values, the bounds for time separation become closer, or equivalently, the time sequence becomes more uniform. We can observe this effect in (6) where amplitude is approximately a scaled version of the time axis.

D. Iterative Algorithm for the Realization of M_α

In this section, we propose an iterative algorithm for the implementation of M_α to generate $h(u)$ from $f(t)$. By duality, an equivalent algorithm can be used for the implemention of $M_{\alpha^{-1}}$ to generate $f(t)$ from $h(u)$. For ease of illustration, we consider a modified version of the transformation M_α defined in (7) which we denote by $\tilde{M}_\alpha$:

$$\begin{aligned} f(t) &= \tilde{h}(\frac{1}{\alpha} f(t) + t) \\ \tilde{h}(u) &= f(-\frac{1}{\alpha}\tilde{h}(u) + u). \end{aligned} \tag{7}$$

Equations (7) form the basis for the iterative algorithm formalized in the following theorem.

Theorem 1: Let the function f be Lipschitz continuous with constant $< \alpha$ and suppose that $\sup_{t\in\mathbb{R}} |f(t)| \leq A$. Then, the function $\tilde{h}(u) = (\tilde{M}_\alpha f)(u)$ for $u \in \mathbb{R}$ can be obtained by the iteration

$$\tilde{h}_{n+1}(u) = f(u - \frac{1}{\alpha}\tilde{h}_n(u)) \tag{8}$$

for $n \geq 0$ where $\tilde{h}_0(u) = f(u)$ and $\tilde{h}_n(u) \to \tilde{h}(u)$ as $n \to \infty$.

The detailed proof is carried out in Appendix A.

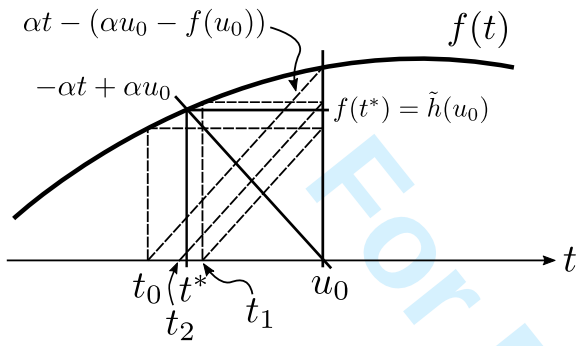

Fig. 5. Illustration of the iteration described in Theorem 1 with the initialization $t_0 = u_0$.

As used in the preceding, the value of $\tilde{h}(u_0)$ can be obtained from the first equality in (7). In particular, $\tilde{h}(u_0) = f(t^*)$ where t^* is the value that satisfies $u_0 = t^* + f(t^*)/\alpha$. The solution is unique since the slope of the ramp, in absolute value, is always greater than the maximum value of the derivative of f. As shown in Fig. 5, t_0 is the time instant at which the ramp $\alpha t_0 - \alpha t$ intersects the function $f(t)$. In the same way, the value of the $(n+1)$-th iteration can be viewed as the solution of $\alpha t - (\alpha u_0 - f(t_n)) = 0$. In other words, we iteratively construct a straight line passing through the point $(u_0, f(t_n))$. The intersection with the horizontal axis then corresponds to the value of t_{n+1}.

IV. Spectral Properties

Assumptions made on the source signal f are naturally reflected in the structure of h. In this section, we assume that f is a bandlimited function and derive properties regarding the spectral content of the amplitude-time function h. The duality between f and $h = M_\alpha f$ implies that similar conclusions can be made about f when h is assumed to be bandlimited.

As an example to motivate the discussion, consider the bandlimited input signal $f(t) = \mathrm{sinc}(t)$ to produce $h = M_\alpha f$ where α is assumed to be positive and large enough so that $g(t) = f(t) + \alpha t$ is strictly monotonic. Fig. 6 depicts both functions f and h. Note that h presents shear-like behavior relative to to the shape of f. This effect is caused by the subtraction of a ramp from the parts of g where its derivative is small. Since, the derivative of g^{-1} is the reciprocal of g, these regions also correspond to large values of the derivative of h. This structure may entail the presence of relevant energy at high frequencies. In particular, we could expect that the frequency-domain characteristics of h are roughly controlled by the difference $\alpha - B$ for $|f'(t)| \leq B$.

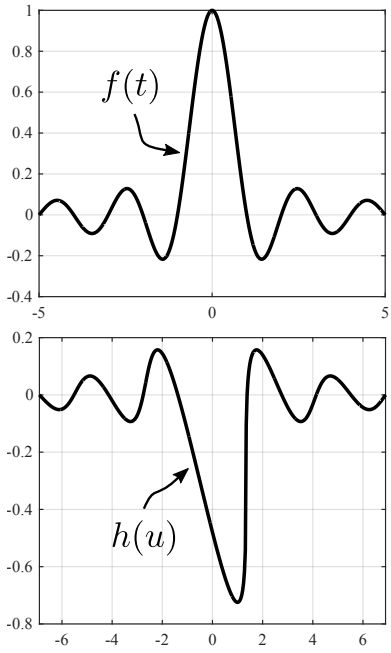

Fig. 6. Example of the transformation in amplitude sampling where $f(t) = \mathrm{sinc}(t)$, $\alpha = 1.38$, and $h = M_\alpha f$.

In exploring the spectral content of h we assume that f is bandlimited to σ rad/s with $\sigma > 0$ and bounded in amplitude, i.e. $|f(t)| < A$ for some A. We further assume that the decay of $f(t)$ for t real satisfies $|f(t)| \leq A/(1+t^2)$. In principle, the extension to square-integrable functions is straightforward. With our assumptions on f, Bernstein's inequality [26] provides the bound $|f'(t)| \leq A\sigma$ for all $t \in \mathbb{R}$. This bound gurantees that the function u defined as

$$u = g(t) = \alpha t + f(t). \tag{9}$$

will be strictly monotonic whenever $|\alpha| > A\sigma$. The function h is then given by $h(u) = g^{-1}(u) - u/\alpha$. From Theorem 2 below it follows that the decay of the Fourier transform of h, denoted by $\hat{h}(\xi)$ for ξ in Hz, satisfies $\hat{h}(\xi) = \mathcal{O}(e^{-2\pi|\xi|b})$ as $\xi \to \infty$ where $b > 0$ is determined by the difference $|\alpha| - A\sigma$.

Theorem 2: Let $f(t) : \mathbb{R} \to \mathbb{R}$ be a continuous function bandlimited to $\sigma > 0$ rad/s. Assume further that $|f(t)| \leq A/(1+t^2)$ for all $t \in \mathbb{R}$ and some $A > 0$. Construct the function

$$u = g(t) = \alpha t + f(t) \tag{10}$$

for $|\alpha| > A\sigma$. Then, there exists $g^{-1}(u)$ for all $u \in \mathbb{R}$ and a constant $C > 0$ such that the Fourier transform of $h(u) = g^{-1}(t) - u/\alpha$ satisfies $|\hat{h}(\xi)| \leq Ce^{-2\pi|\xi|b}$ for any $0 \leq b < a$ such that

$$a = \frac{|\alpha|}{\sigma}\log\left(\frac{|\alpha|}{A\sigma}\right) - \frac{|\alpha| - A\sigma}{\sigma}. \tag{11}$$

and $\xi \in \mathbb{R}$.

The detailed proof is carried out in Appendix B.

As anticipated, the rate of decay of the Fourier transform at infinity depends on $|\alpha| - A\sigma$. The difference is logarithmic in the first term and linear in the second one. The larger the difference the faster the decay at infinity. Note that $a > 0$ always holds since $|\alpha| > A\sigma$. Assuming $\alpha > 0$, this

difference is precisely impacting the highest slope portions in h, or, equivalently, the regions in which f' is smallest. The underlying reason being that the derivative of g^{-1} is the reciprocal of g, i.e. $(g^{-1}(u))' = 1/g'(g^{-1}(u))$ for all $u \in \mathbb{R}$. Informally, it is the tilted regions in the shape of h are responsible, to some extent, for the high-frequency content.

It should be emphasized that any bandlimited function will naturally be in the class of signals whose spectrum exhibits at least exponential decay at infinity. However, Theorem 3 stated below asserts that f and h cannot be simultaneously bandlimited. The precise statement in the description of the theorem guarantees this property with the possible exception of, at most, one value of α. For practical purposes, we can ignore this isolated case.

Theorem 3: Under the conditions of Theorem 2 and unless f is constant, the function $h(u)$ is nonbandlimited for every $\alpha > A\sigma$ with at most one exception.

The detailed proof is carried out in Appendix C.

In the singular case, in which f is a constant, it can be shown through the constructive process of M_α by ramp addition that h is constant as well, specifically, for $f = A$, then $h = -A/\alpha$. From another point of view, according to (1), the function f results, in general, from h with a nonlinear warping of the independent variable. When either of the two functions is constant, the warping is affine. Therefore, in this case, the bandlimited property is preserved [27]. In our context the conclusion follows directly from (1) that if either f or h is constant, the other must be also.

More generally, if $|\alpha|$ increases significantly, the warping function becomes approximately linear since $f(t)$ is negligible compared to αt, i.e. $f(t) \approx -\alpha h(\alpha t)$. This is consistent with (11) where an increase of $|\alpha|$ produces a faster decay at infinity of $\hat{h}$.

V. Time-Domain Decay Properties

In some sense, h inherits characteristics of f since it is a "time-warped" version of f. In this section, we show the connections between the properties of f and h in the time domain with the relationship between f and h as specified in (1) which explicitly requires that the slope of the ramp added to f and the slope of the ramp subtracted to obtain h be exact inverses. Intuitively, it is not surprising that the function h should present decay properties similar to those of f once the unbounded growth of the ramp component has been subtracted. In particular, it is stated in [28, Chapter 2, Proposition 1] that when the slopes of the two ramps as inverses, the decay of h will match that of f. Otherwise h does not decay appropriately on the real line.

The transformation M_α also has an impact on the L^p norms of the respective functions with the parameter α playing a crucial role. It can be shown that the decay on the real line of both functions is related by [28, Chapter 2, Proposition 3]

$$||h||_p = \frac{1}{\alpha^{1-\frac{1}{p}}}||f||_p, \ p \in [1, \infty]. \tag{12}$$

Not only does h belong to $L^p(\mathbb{R})$ if f does, but their respective norms are also related by a scaling factor which is precisely α. Indeed, for very large values of $|\alpha|$, the ramp approaches the vertical axis, thus reducing the range of h and decreasing the norm.

In terms of a sense of distance, let f_1 and f_2 generate h_1 and h_2 respectively. The transformation M_α preserves the L^1 distance [28, Chapter 2, Proposition 4], i.e.

$$||h_1 - h_2||_1 = ||f_1 - f_2||_1. \tag{13}$$

By duality, these properties hold irrespective of the role of each function as an input or output.

VI. Reconstruction in Amplitude Sampling

Amplitude sampling can be interpreted as signal-dependent nonuniform time sampling of the source signal f based on uniform time sampling of the associated amplitude-time function h. If f is bandlimited, then as was shown in Section IV h is not bandlimited and consequently cannot be exactly reconstructed through bandlimited interpolation. Our reconstruction approach begins by initially using sinc interpolation as an approximation. This is then extended to an iterative algorithm that achieves accurate recovery. Throughout this entire section, we assume that the source signal f is bandlimited to σ rad/s, and $|f(t)| \leq A/(1+t^2)$ for $A > 0$ and all $t \in \mathbb{R}$.

A. Bandlimited Interpolation Algorithm (BIA)

The approximate reconstruction of f based on sinc interpolation of h is depicted in Fig. 7. From this approximation to h an approximation to f is generated through $M_{\alpha^{-1}}$ which is then lowpass filtered since f is assumed to be bandlimited. In particular, the D/C system is defined by the relationship

$$h_\Delta(u) = \sum_{k \in \mathbb{Z}} h(k\Delta)\mathrm{sinc}(u/\Delta - k). \tag{14}$$

Note that the samples of h are related to $\{t_n\}$ as $h(n\Delta) = t_n - n\Delta/\alpha$, $n \in \mathbb{Z}$. At this stage the approximation can be quantified as [28, Chapter 3, Proposition 6]

$$||h - h_\Delta||_\infty \leq \frac{C'}{a} e^{-\pi \frac{a}{\Delta}}. \tag{15}$$

The error in (15) is then controlled both by the difference $|\alpha| - A\sigma$ and the quantization step size Δ. As already discussed, increasing the difference $|\alpha| - A\sigma$ produces, in some sense, a function h with a faster high-frequency spectral decay and therefore one that is more approximately bandlimited. Thus, we would expect that the performance of the approximation can be improved by increasing this difference.

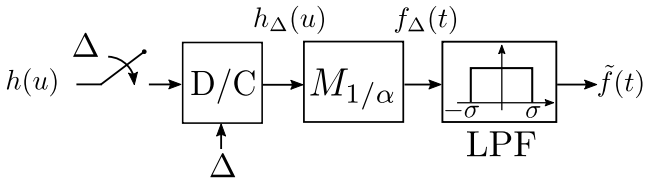

Fig. 7. Approximate reconstruction procedure for a bandlimited source signal f such that $h = M_\alpha f$. The block D/C is a discrete-to-continuous operation involving sinc interpolation with period Δ.

B. Iterative Amplitude Sampling Reconstruction (IASR)

The bandlimited interpolation algorithm (BIA) forms the basis for an iterative algorithm which we refer to as the Iterative Amplitude Sampling Reconstruction (IASR) algorithm illustrated in Fig. 8. Note that if the initialization satisfies $h_0(u) \equiv 0$ and $f_0(t) \equiv 0$, the first iteration corresponds precisely to BIA, i.e. $f_1(t) = \tilde{f}(t)$. Similar to the approximate bandlimited recovery, the emphasis is placed on the reconstruction of h from its nonuniform amplitude samples and then imposing the bandlimited constraint on the successive approximations to f with the objective of iteratively reducing the error $||e_k(t)||_2$.

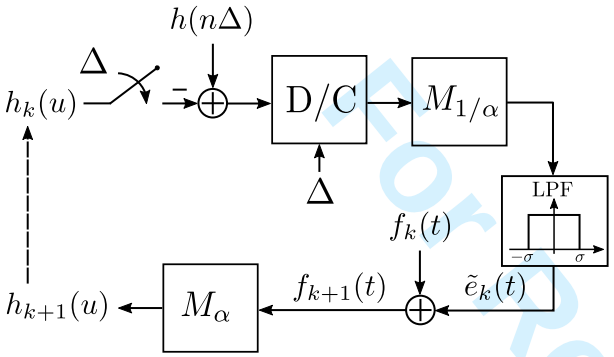

Fig. 8. Block diagram representation of the iterative amplitude sampling reconstruction (IASR) algorithm.

C. Simulation Results

In all of the simulations in this section, the source signal f is chosen as white noise bandlimited to σ rad/s and bounded by $A > 0$. The quantization step size Δ and the parameter α are chosen so that the sampling density is greater or equal than the Landau rate [25], which, in our case, is given by π/σ. We choose as a measure of approximation error the signal-to-error ratio (SER) given by

$$\mathrm{SER} = 10\log_{10}\left(\frac{||f_k||_2^2}{||f - f_k|_2^2}\right) \tag{16}$$

where f_k is the k-th iteration.

Since amplitude sampling also implies nonuniform time sampling on the source signal f, we also directly apply a nonuniform reconstruction algorithm to recover f. Specifically, we compare IASR to the Voronoi method developed in [29, Theorem 8.13]. Based on the bounds in (6) for the time instants, it is straightforward to see that the sampling instants in an amplitude sampling setting satisfy the requirements of the Voronoi method for an appropriate choice of the parameters. In particular, it can be shown that it is sufficient that

$$\frac{\Delta}{|\alpha| - A\sigma} > \frac{\pi}{\sigma}. \tag{17}$$

In initializing both algorithms, the 0-th iteration in both IASR and the Voronoi method is assumed to be zero.

In Fig. 9, we have modified individually the parameters α or Δ. In reducing the value of the quantization step size Δ, the transformed function $\alpha t + f(t)$ will clearly cross more

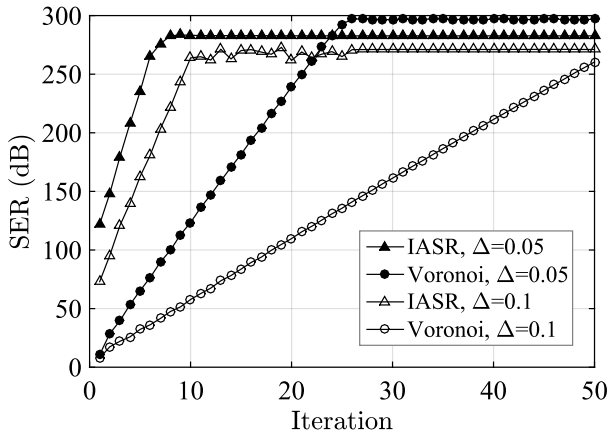

(a)

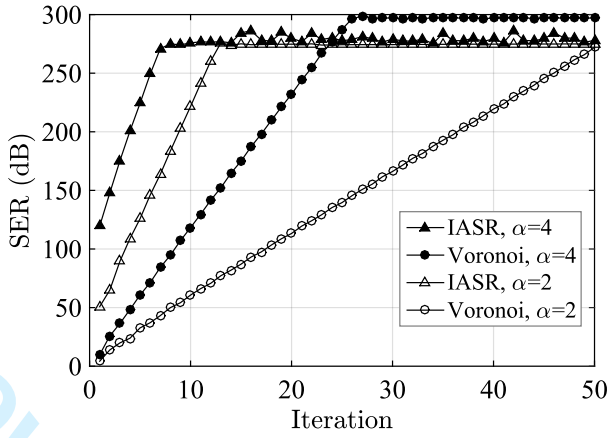

(b)

Fig. 9. Performance comparison between IASR, AWM, and BIA, for a broadband input signal bandlimited and bounded; (a) Δ is changed while α is fixed; (b) α is changed while Δ is fixed.

amplitude levels per unit of time. Similarly, when the slope of the ramp added to f is increased in absolute value, it also causes an increase in the level-crossing density. Thus, both effects result in an increase of the sampling density, and, as shown in the figure, the rate of convergence improves. However, it can be observed that the rate of convergence is faster in the IASR case. The first iteration in IASR achieves a better approximation than the Voronoi method although the rate of convergence appears to be highly insensitive to this change of parameters. On the other hand, the Voronoi method is significantly impacted by the change in sampling density. Moreover, it requires several iterations until it obtains the same approximation performance as the first iteration in IASR. As shown in Fig. 10 the same conclusions hold if we increase the oversampling ratio by considering signals with smaller bandwidths and, at the same time, keeping α and Δ fixed.

Thus far, we have focused on modifying the sampling density. Additionally, due to the structure of the sampling process in amplitude sampling, it is also possible to keep the sampling density fixed while changing both α and Δ accordingly. The rate of convergence in the Voronoi method

is determined by the maximal separation between consecutive sampling instants. With constant sampling density, the performance of the Voronoi method does not change, as shown in Fig. 11. However, IASR presents an improvement in the rate of convergence. This is not surprising since the difference $|\alpha| - A\sigma$ has increased, which likely results in a better approximation of the sinc interpolation in IASR.

When the input signal is highly oversampled, we have empirically observed that the Voronoi method has a faster rate of convergence. Nevertheless, when the sampling instants become increasingly sparse approaching the Landau rate, IASR performs significantly better.

In summary, overall, IASR appears to have better performance than the Voronoi method in terms of speed of convergence when the sampling density approaches the Landau rate. Changes in the sampling density have a higher impact on the convergence in the Voronoi method than in IASR. Moreover, IASR performance can also be improved by increasing the difference $|\alpha| - A\sigma$ while keeping the sampling density invariant. In [24], a scaling of the input signal also produces an increase in the speed of convergence. This performance improvement of IASR over the Voronoi method may be due to the characteristics of the sampling instants. Specifically the sampling instants in IASR inherently incorporate the amplitude sampling structure and therefore contain more information initially than more general nonuniform sampling would. In some sense, this may suggest that IASR is designed to more effectively exploit the structure of this particular sampling process which implicitly is signal dependent and consequently signal information is implicitly embedded in both the sampling times and the sample values.

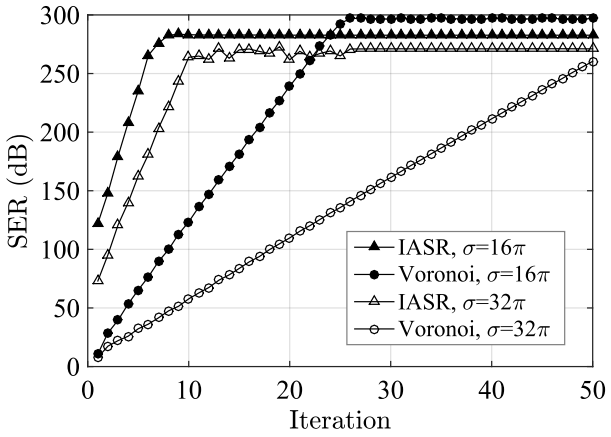

Fig. 10. Performance comparison between IASR and the Voronoi method when the bandwidth σ is changed, and α and Δ are fixed.

VII. Conclusion

Amplitude sampling represents a signal with equally-spaced amplitude values and infinite-precision timing information by reversibly transforming the source signal. This transformation provides the perspective of viewing amplitude sampling as uniform sampling of an associated amplitude-time function or equivalently as nonuniform time sampling of the source signal.

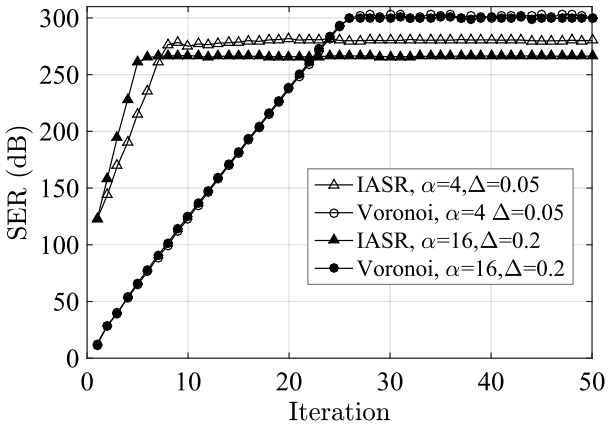

Fig. 11. Performance comparison between IASR and the Voronoi method when the sampling density is fixed and α and Δ are changed.

The properties of both functions are connected by a duality relationship. Similarly, an iterative algorithm for recovery was proposed and evaluated that exploits the particular characteristics of the sampling instants in amplitude sampling. For the amplitude sampling structure this algorithm outperforms the use of more general nonuniform reconstruction algorithms.

Appendix A
Proof of Theorem 1

According to (7), obtaining $\tilde{h}(u_0)$ for some fixed $u_0 \in \mathbb{R}$ is equivalent to finding some $t^* \in \mathbb{R}$ such that $u_0 = t^* + f(t^*)/\alpha$ since $\tilde{h}(u_0) = f(t^*)$. Therefore, we have to find the roots of

$$t = u_0 - \frac{1}{\alpha} f(t) \triangleq v_{u_0}(t) \tag{18}$$

for $t \in \mathbb{R}$. It is easy to see that $v_{u_0}(t)$ is Lipschitz continuous for some constant $K < 1$. Furthermore, there always exists some $\epsilon \geq A/\alpha$ such that $v_{u_o} : I \to I$ where $I = [u_0 - \epsilon, u_0 + \epsilon]$. Thus, the Banach fixed-point theorem [30] guarantees the uniqueness and existence of a solution. Moreover, it ensures convergence with the following bounds for the error

$$|t_{n+1} - t^*| \leq K|t_n - t^*| \tag{19}$$

for $n \geq 0$ where $t_0 \in I$ and $t_{n+1} = v_{u_0}(t_n)$. Then, the iteration can be equivalently expressed in terms of the functional composition form as

$$\tilde{h}_{n+1}(u_0) = f(u_0 - \frac{1}{\alpha}\tilde{h}_n(u_0)). \tag{20}$$

Since u_0 was chosen arbitrarily, the same conclusions hold for any $u_0 \in \mathbb{R}$. □

Appendix B
Proof of Theorem 2

We first introduce several results that will become useful in the proof of the theorem. Define the open disk in the complex plane centered at z_o and of radius r as

$$D_r(z_o) = \{z \in \mathbb{C} : |z - z_o| < R\} \tag{21}$$

and use $\overline{D}_r(z_o)$ for its closure.

Lemma 1: Let f be a holomorphic function in some region Ω with power series $f(z) = \sum_{n=0}^{\infty} a_n (z - z_o)^n$ at $z_o \in \Omega$. Consider a disk of radius R centered at z_o such that Ω contains the disk and its closure. If $a_1 \neq 0$ and

$$|a_1| > \sum_{n=2}^{\infty} |a_n| n R^{n-1}, \tag{22}$$

then f is injective in any open disk of radius $r \leq R$.

Proof 1: Without loss of generality assume $z_o = 0$, thus the power series expansion of f around the origin is given by $f(z) = \sum_{n=0}^{\infty} a_n z^n$ for all $z \in \Omega$. Take $z_1, z_2 \in \overline{D}_R(0) \subset \Omega$ such that $z_1 \neq z_2$ and recall that for any $z, w \in \mathbb{C}$ the following identity holds

$$(z^n - w^n) = (z - w)(z^{n-1} + z^{n-2} w + \ldots + z w^{n-2} + w^{n-1}). \tag{23}$$

We can write

$$\begin{aligned} \left| \frac{f(z_2) - f(z_1)}{z_2 - z_1} \right| &= \left| a_1 + \sum_{n=2}^{\infty} a_n \frac{z_2^n - z_1^n}{z_2 - z_1} \right| \\ &= \Big| a_1 + \sum_{n=2}^{\infty} a_n (z_2^{n-1} + z_2^{n-2} z_1 + \ldots \\ &\qquad \ldots + z_2 z_1^{n-2} + z_1^{n-1}) \Big| \\ &\geq |a_1| - \sum_{n=2}^{\infty} |a_n| n R^{n-1}. \end{aligned}$$

where the last inequality follows from the reverse triangle inequality and the fact that $|z_1|, |z_2| \leq R$. Thus, if $|a_1| - \sum_{n=2}^{\infty} |a_n| n R^{n-1} > 0$, then $f(z_2) - f(z_1) \neq 0$ and $f(z)$ is injective in $D_r(z_o)$ for any $r \leq R$. □

Proposition 1: Let $f : U \to V$ be a bijective continuous function. Consider a set Ω such that its closure $\overline{\Omega}$ is strictly contained in U, then $f(\partial\Omega) = \partial f(\Omega)$.

Proof 2: Consider $x \in \partial\Omega$, which is clearly a limit point of Ω. We know there exist a convergent sequence $x_n \to x$ for $n \geq 1$, where $x_n \in \Omega$. By continuity, we have that $f(x_n) \to f(x)$ is a convergent sequence in V. As f is a bijection from U to V, we have that $f(x_n) \neq f(x)$ for all $n \geq 1$, thus $f(x) \in \overline{f(\Omega)}$. Moreover, $f(x) \neq f(x')$ for all $x' \in \Omega$, therefore $f(x) \in \partial f(\Omega)$ for all $x \in \partial\Omega$. It follows that $f(\partial\Omega) \subseteq \partial f(\Omega)$.

Now, we claim that for every $y \in \partial\Omega$ there exists an $x \in \partial\Omega$ such that $y = f(x)$. Imagine this is not true and there exists an $x_o \in U \setminus \partial\Omega$ such that $y_o = f(x_o)$. From our previous discussion, it is clear that x_o cannot be in Ω, then imagine $x_o \in U \setminus \overline{\Omega}$. Since f is continuous and bijective, we can choose a sufficiently small $\epsilon > 0$ such that $f^{-1}(D_\epsilon(y_o)) \subset D_\delta(x_o)$ and $D_\delta(x_o) \cap \overline{\Omega} = \emptyset$ for some $\delta > 0$. However, as y_o is a point in the boundary, it holds that $D_\epsilon(y_o) \cap f(\Omega) \neq \emptyset$. Thus, there exist an $x_1 \in \Omega$ such that $f(x_1) = y'$ for some $y' \in D_\epsilon(y_o)$. At the same time, there also exists an $x_2 \in f^{-1}(D_\epsilon(y_o))$ such that $f(x_2) = y'$, where $x_1 \neq x_2$. This contradicts the bijectivity assumption, thus $f(\partial\Omega) \supseteq \partial f(\Omega)$ which together with $f(\partial\Omega) \subseteq \partial f(\Omega)$ gives $f(\partial\Omega) = \partial f(\Omega)$. □

Proposition 2: Suppose $f(z)$ is an entire function of exponential type σ such that $|f(x)| \leq A/(1 + x^2)$ for all $x \in \mathbb{R}$. Then, the following bound holds for all $z \in \mathbb{C}$

$$|f(z)| \leq \frac{A e^{\sigma |y|}}{1 + x^2}. \tag{24}$$

Proof 3: By assumption, we have that $|f(z)| \leq A e^{\sigma |z|}$ for all $z \in \mathbb{C}$. Construct the function $F(z) = (1/A)(1 + x^2) e^{i\sigma z} f(z)$, then F is bounded by 1 on the positive imaginary and positive real axis. If we consider the first quadrant $Q = \{z = x + iy : x > 0, y > 0\}$, it is clear that there exists constants $C, c > 0$ such that $|F(z)| \leq C e^{c|z|}$ for $z \in Q$. We conclude by the Phragmén-Lindelöf theorem that $|F(z)| \leq 1$ for all z in Q. This implies that $|f(z)| \leq A e^{\sigma y}/(1 + x^2)$ for $z \in Q$. Using the same argument, one can show that the same is true in the second quadrant. For the third and fourth quadrants we use instead the function $F(z) = (1/A)(1 + x^2) e^{-i\sigma z} f(z)$, which shows that (24) also holds for $y \leq 0$. □

The function f is of moderate decrease. By the Paley-Wiener theorem, its Fourier transform is then supported on $[-M, M]$. Thus, Bernstein's inequality implies that $|f'(x)| \leq \sigma A$. Now, we can split the proof of the theorem in three steps.

Step 1. We claim that the function $u = g(x) = \alpha x + f(x)$ admits a real analytic inverse function whenever $\alpha > \sigma A$. It is clear that $g(x)$ is analytic for all $x \in \mathbb{R}$ since it is the sum of two analytic functions on the whole real line. Moreover, $g(x)$ is a strictly increasing monotone function because $|f'(x)| \leq A\sigma$ and $\alpha > A\sigma$, which implies $g'(x) > 0$. The Real Analytic Inverse Function theorem guarantees that for a point x_o where $g'(x_o) \neq 0$, there exists a neighborhood J_o of x_o and a real analytic function g^{-1} defined on an open interval I_o containing $g(x_o)$ satisfying $(g^{-1} \circ g)(x) = x$ for $x \in J_o$ and $(g \circ g^{-1})(u) = u$ for $y \in I_o$. Since $g'(x) \neq 0$ for all real x, it is always possible for any given $x_1 \in \mathbb{R}$ to find an $x_2 \notin J_1$ such that $J_1 \cap J_2 \neq \emptyset$. Thus, by analytic continuation, we conclude that $g^{-1}(u)$ is analytic on the whole real line.

Step 2. We show that the function $g^{-1}(w)$ is analytic in a region containing the horizontal strip

$$\begin{aligned} S_a = \{ & w \in \mathbb{C} : |\mathrm{Im}(w)| < a, \\ & \text{where } a = \frac{\alpha}{\sigma} \log\left(\frac{\alpha}{\sigma}\right) - \frac{\alpha - \sigma}{\sigma} \}. \end{aligned} \tag{25}$$

The function $g(z) = \alpha z + f(z)$ is an entire function of exponential type σ and admits a power series expansion around $x \in \mathbb{R}$

$$g(z) = \alpha z + \sum_{n=0}^{\infty} \frac{f^{(n)}(x)}{n!} (z - x)^n \tag{26}$$

for all $z \in \mathbb{C}$. By Bernstein's inequality, the derivatives of f are bounded on the real line by $|f^{(n)}(x)| \leq A\sigma^n$. We now look for a region where $g(z)$ is injective. Using Lemma 1, $g(z)$ is injective in a disk of radius $R > 0$ whenever

$$|\alpha + f'(x)| > \frac{A}{R} \sum_{n=2}^{\infty} n \frac{(\sigma R)^n}{n!} = A\sigma(e^{R\sigma} - 1) \tag{27}$$

or, equivalently

$$R < \frac{1}{\sigma} \log\left(1 + \frac{|\alpha + f'(x)|}{A\sigma}\right). \tag{28}$$

The right-hand side of this expression is lower bounded by $(1/\sigma)\log(1+(\alpha-A\sigma)/A\sigma) > 0$, since $|f'(x)| \leq A\sigma < \alpha$ for all $x \in \mathbb{R}$. Thus, it is always possible to choose a disk of positive radius satisfying this lower bound such that $g(z)$ is injective.

Let us fix an R satisfying this lower bound. Remember that holomorphic functions are open mappings, i.e. they map open sets to open sets. Thus, $g(z)$ maps an open disk of radius R to the open set $g(D_R(x))$. By continuity, $g(D_R(x))$ is also connected since $D_R(x)$ is connected. Therefore, the mapping $g(z) : D_R(x) \to g(D_R(x))$ represents a holomorphic bijection, thus its inverse is also holomorphic. Moreover, the inverse agrees with $g^{-1}(u)$ for real $u \in g(D_R(x))$. Thus, it represents the analytic continuation of $g^{-1}(u)$ on $u \in g(D_R(x))$. In fact, we can always choose a disk $D_R(x')$ such that $g(D_R(x)) \cap g(D_R(x')) \neq \emptyset$, where the inverse functions defined on their respective images take the same value in the intersection for real u. Again, by analytic continuation, we can analytically extend $g^{-1}(u)$ to $g(D_R(x)) \cup g(D_R(x'))$. Repeating this process for all real x, we obtain the analytic continuation of $g^{-1}(u)$ in the open set $\Omega = \cup_{x\in\mathbb{R}} g(D_R(x))$.

We want to find an $a > 0$ such that $S_a \subseteq \Omega$. Using Lemma 1, the boundary of the disk $\partial D_R(x)$ is mapped bijectively to $\partial g(D_R(x))$. Therefore, the largest radius ρ for a disk centered at $g(x)$ such that $D_\rho(g(x)) \subseteq g(D_R(x))$ for all $x \in \mathbb{R}$ is given by

$$\rho = \inf_{x\in\mathbb{R}} \sup_{|z-x|=R} \{|g(z)-g(x)| : D_{|g(z)-g(x)|}(g(x)) \subseteq g(D_R(x))\}. \tag{29}$$

We can use the power series expansion of g around x to find a lower bound for ρ in the following manner

$$\begin{aligned} |g(z)-g(x)| &= |\alpha(z-x) + \sum_{n=1}^{\infty} a_n (z-x)^n| \\ &\geq \alpha R - \sum_{n=1}^{\infty} \frac{A\sigma^n}{n!} R^n = \alpha R - A(e^{R\sigma}-1). \end{aligned}$$

for $|z-x| = R$. The right-hand side of the last expression represents a strictly concave function of R, thus the maximum is achieved for

$$R = \frac{1}{\sigma}\log\left(\frac{\alpha}{A\sigma}\right) > 0 \tag{30}$$

which is positive as $\alpha > A\sigma$ and satisfies the upper bound in (28). Setting the value of R as in (30), we can write

$$|g(z)-g(x)| \geq \rho \geq \frac{\alpha}{\sigma}\log\left(\frac{\alpha}{A\sigma}\right) - \left(\frac{\alpha-A\sigma}{\sigma}\right) \tag{31}$$

for all $x \in \mathbb{R}$ and $|z-x| = R$. This implies that $S_a \subseteq \Omega$ for any a such that

$$a < \frac{\alpha}{\sigma}\log\left(\frac{\alpha}{A\sigma}\right) - \left(\frac{\alpha-A\sigma}{\sigma}\right). \tag{32}$$

Step 3. We show that $h(w)$ is of moderate decay on each horizontal line $|\mathrm{Im}(w)| < a$, uniformly in $|y| < a$. First, we note that since f is an entire function of exponential type σ and is of moderate decrease along the real line, by Proposition 2

$$|f(z)| \leq \frac{Ae^{\sigma|y|}}{1+x^2} \tag{33}$$

for all $z \in \mathbb{C}$. Let us now fix an R satisfying (30), then we have a bijection from $D_R(x')$ to $g(D_R(x'))$ for some $x' \in \mathbb{R}$. Therefore, $z = g^{-1}(w)$, where $w \in g(D_R(x))$ and $z \in D_R(x')$. Since $|y| < R$ for $z \in D_R(x')$, we also have $|f(z)| = |\alpha z - g(z)| \leq Ae^{\sigma R}/(1+x^2)$, or equivalently

$$|w - \alpha g^{-1}(w)| \leq \frac{Ae^{\sigma R}}{1+(g^{-1}(u))^2} \tag{34}$$

whenever $w \in g(D_R(x))$ and $z \in D_R(x')$. Using the reverse triangle inequality in the previous expression for real w, we can also obtain

$$|g^{-1}(u)| \geq \frac{|u|}{\alpha} - \frac{Ae^{\sigma R}}{\alpha}. \tag{35}$$

which is true for all $u \in \mathbb{R}$ since $x = g^{-1}(u)$ holds for all real x and u as shown in the first step of the proof. Define the function for all real u

$$\psi(u) = \begin{cases} |u|/\alpha - Ae^{\sigma R}/\alpha & \text{if } |u|/\alpha > Ae^{\sigma R}/\alpha \\ 0 & \text{otherwise} \end{cases} \tag{36}$$

which clearly satisfies $|g^{-1}(u)| \geq |\psi(u)|$. Make $\beta = 1/\alpha$ and multiply both sides of (34) by $1/\alpha$ to see that $|h(w)| = |w/\alpha - g^{-1}(w)|$. Combining these expressions, we can then write for some $A' > 0$ and $w \in g(D_R(x'))$

$$|h(w)| \leq \frac{Ae^{\sigma R}/\alpha}{1+g^{-1}(u)^2} \leq \frac{Ae^{\sigma R}/\alpha}{1+\psi(u)^2} \leq \frac{A'}{1+u^2} \tag{37}$$

As our choice of x' was arbitrary, this is true for any $x' \in \mathbb{R}$ and $|h(u+iv)|$ is of moderate decrease along horizontal lines.

Therefore, the function $h(w)$ is analytic on the strip S_a and it is of moderate decrease on each horizontal line $|\mathrm{Im}(w)| = v$, uniformly in $|v| < a$, as long as $\beta = 1/\alpha$. By the Paley-Wiener theorem [31, Theorem X], we conclude that there exists a constant $C > 0$ such that $|\hat{h}(\xi)| \leq e^{-2\pi b\xi}$ for any $0 \leq b < a$. □

APPENDIX C
PROOF OF THEOREM 3

Construct the function $g(z) = \alpha z + f(z)$ where f is not constant. By Picard's little theorem, there exists at most one value $\alpha > A\sigma$ that $f'(z)$ does not take. For the rest of them, there always exists a $z_o \in \mathbb{C}$ such that $g'(z_o) = \alpha + f'(z_o) = 0$. Then, it is possible to write

$$g(z) - a_0 = (z-z_o)^2[a_2 + a_3(z-z_o) + a_4(z-z_o)^2 + \ldots]. \tag{38}$$

Therefore, the function $g(z) - z_o$ has a zero of order ≥ 2 at z_o. By the Local Mapping Theorem, g is n-to-1 near z_o for $n \geq 2$. Using the argument of analytic continuation of local biholomorphisms in Theorem 2, we conclude that the analytic extensions of h around $g(z_o)$ are multivalued. This excludes the possibility of h being entire, thus, h cannot be bandlimited. If $f(z) = C$ for some $C > 0$, then $h(u) = -C/\alpha$, which is bandlimited in the distributional sense. □

REFERENCES

[1] E. T. Whittaker, "XVIII.—On the functions which are represented by the expansions of the interpolation-theory," *Proceedings of the Royal Society of Edinburgh*, vol. 35, pp. 181–194, 1915.
[2] V. A. Kotelnikov, "On the carrying capacity of the ether and wire in telecommunications," in *Material for the First All-Union Conference on Questions of Communication, Izd. Red. Upr. Svyazi RKKA, Moscow*, 1933.
[3] C. E. Shannon, "Communication in the presence of noise," *Proceedings of the IRE*, vol. 37, no. 1, pp. 10–21, 1949.
[4] F. Bond and C. Cahn, "On sampling the zeros of bandwidth limited signals," *IRE Transactions on Information Theory*, vol. 4, no. 3, pp. 110–113, 1958.
[5] B. F. Logan, "Information in the zero crossings of bandpass signals," *Bell System Technical Journal*, vol. 56, no. 4, pp. 487–510, 1977.
[6] S. Roweis, S. Mahajan, and J. Hopfield, "Signal reconstruction from zero-crossings," August 1998, draft (accessed May 2016) https://www.cs.nyu.edu/ roweis/papers/logan.ps.
[7] S. J. Haavik, "The conversion of the zeros of noise," Master's thesis, University of Rochester, Rochester, NY, 1966.
[8] I. Bar-David, "An implicit sampling theorem for bounded bandlimited functions," *Information and Control*, vol. 24, no. 1, pp. 36–44, 1974.
[9] R. Kumaresan and Y. Wang, "A new real-zero conversion algorithm," in *Proceedings 2000 IEEE International Conference on Acoustics, Speech, and Signal Processing.*, vol. 1, 2000, pp. 313–316 vol.1.
[10] R. J. Duffin and A. C. Schaeffer, "Some properties of functions of exponential type," *Bulletin of the American Mathematical Society*, vol. 44, no. 4, pp. 236–240, 1938.
[11] E. M. Stein and R. Shakarchi, *Complex analysis*, ser. Princeton Lectures in Analysis, II. Princeton University Press, Princeton, NJ, 2003.
[12] J. Selva, "Efficient sampling of band-limited signals from sine wave crossings," *IEEE Trans. Signal Processing*, vol. 60, no. 1, pp. 503–508, 2012.
[13] S. Kay and R. Sudhaker, "A zero crossing-based spectrum analyzer," *IEEE Transactions on Acoustics, Speech and Signal Processing*, vol. 34, no. 1, pp. 96–104, 1986.
[14] T. V. Sreenivas and R. J. Niederjohn, "Zero-crossing based spectral analysis and svd spectral analysis for formant frequency estimation in noise," *IEEE Transactions on Signal Processing*, vol. 40, no. 2, pp. 282–293, 1992.
[15] R. Kumaresan and N. Panchal, "Encoding bandpass signals using zero/level crossings: a model-based approach," *Audio, Speech, and Language Processing, IEEE Transactions on*, vol. 18, no. 1, pp. 17–33, 2010.
[16] S. Mallat, "Zero-crossings of a wavelet transform," *IEEE Transactions on Information Theory*, vol. 37, no. 4, pp. 1019–1033, 1991.
[17] J. W. Mark and T. D. Todd, "A nonuniform sampling approach to data compression," *IEEE Trans. Commun.*, vol. 29, no. 1, pp. 24–32, 1981.
[18] Y. Tsividis, "Continuous-time digital signal processing," *Electron. Lett.*, vol. 39, no. 21, pp. 1551–1552, 2003.
[19] H. Inose, T. Aoki, and K. Watanabe, "Asynchronous delta-modulation system," *Electron. Lett.*, vol. 2, no. 3, pp. 95–96, 1966.
[20] P. Martinez-Nuevo, S. Patil, and Y. Tsividis, "Derivative level-crossing sampling," *IEEE Transactions on Circuits and Systems II: Express Briefs*, vol. 62, no. 1, pp. 11–15, 2015.
[21] Y. Tsividis, "Event-driven data acquisition and continuous-time digital signal processing," in *Custom Integrated Circuits Conference (CICC), 2010 IEEE*, 2010, pp. 1–8.
[22] A. Zakhor and A. Oppenheim, "Reconstruction of two-dimensional signals from level crossings." *Proceedings of the IEEE*, vol. 78, no. 1, pp. 31 – 55, 1990.
[23] S. R. Curtis and A. V. Oppenheim, "Reconstruction of multidimensional signals from zero crossings." *Journal of the Optical Society of America. A, Optics & Image Science*, vol. 4, pp. 221 – 231, 1987.
[24] H. Lai, "Reconstruction methods for level-crossing sampling," Master's Thesis, EECS, MIT, June 2016.
[25] H. J. Landau, "Necessary density conditions for sampling and interpolation of certain entire functions," *Acta Mathematica*, vol. 117, no. 1, pp. 37–52, July 1967.
[26] S. N. Bernstein, *Leçons sur les propriétés extrémales et la meilleure approximation des fonctions analytiques d'une variable réelle*. Paris, 1926.
[27] S. Azizi, D. Cochran, and J. McDonald, "On the preservation of bandlimitedness under non-affine time warping," in *Proc. Int. Workshop on Sampling Theory and Applications*, 1999.
[28] P. Martínez-Nuevo, "Amplitude sampling for signal representation," Ph.D. dissertation, Massachusetts Institute of Technology, 2016.
[29] H. G. Feichtinger and K. Gröchenig, "Theory and practice of irregular sampling," *Wavelets: mathematics and applications*, pp. 305–363, 1994.
[30] S. Banach, "Sur les opérations dans les ensembles abstraits et leur application aux équations intégrales," *Fund. Math*, vol. 3, no. 1, pp. 133–181, 1922.
[31] R. E. A. C. Paley and N. Wiener, *Fourier transforms in the complex domain*. American Mathematical Soc., 1934, vol. 19.

Pablo Martínez-Nuevo received the *Ingeniero de Telecomunicación* degree from the ETSIT, University of Valladolid, Spain, in 2010 and the M.Sc. degree in Electrical Engineering from Columbia University, NY, in 2012 where he was awarded the Edwin Howard Armstrong Memorial Award. He received the Ph.D. degree in Electrical Engineering and Computer Science from the Massachusetts Institute of Technology (MIT) in 2016 under the supervision of Prof. Alan V. Oppenheim in the Digital Signal Processing Group. He has been a recipient of the Fundación Rafael del Pino Fellowship, Madrid, Spain, for graduate studies at MIT.

Dr. Martínez-Nuevo is currently a Sr. Acoustical Researcher at Bang&Olufsen in Denmark. His research interests lie within the areas of signal and information processing, sampling theory, and learning.

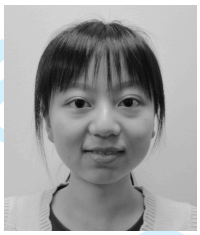

Hsin-Yu Lai received bachelor's degrees in both Electrical Engineering and Mathematics from National Taiwan University in 2014. She received her master's degree in Electrical Engineering and Computer Science (EECS) from the Massachusetts Institute of Technology (MIT) under the supervision of Prof. Alan V. Oppenheim in 2016. During that time, she worked with Dr. Pablo Martínez-Nuevo on amplitude sampling and reconstruction. Hsin-Yu Lai is currently a Ph.D. student in the EECS Department at MIT working with Prof. Vivienne Sze and Prof. Thomas Heldt. Her research interests include signal processing, inference, and algorithm design.

Alan V. Oppenheim (M'65–SM'71–F'77–LF'03) received the S.B. and S.M. degrees in 1961 and the Sc.D. degree in 1964, all in electrical engineering, from the Massachusetts Institute of Technology. He is also the recipient of an honorary doctorate from Tel Aviv University.

In 1964, he joined the faculty at MIT and is currently Professor of Engineering and a MacVicar Fellow. His research interests are in the general area of signal processing, theory, algorithms and its applications. He is coauthor of several widely used textbooks and the editor of several advanced books on signal processing. In Spring 2015, an online version of his Discrete-Time Signal Processing course (6.341) was launched on edX through MIT.

Dr. Oppenheim is a member of the National Academy of Engineering, and a member of Sigma Xi and Eta Kappa Nu. He has been a Guggenheim Fellow and a Sackler Fellow. He has received a number of awards for outstanding research and teaching, including the IEEE Education Medal, the IEEE Jack S. Kilby Signal Processing Medal, the IEEE Centennial Medal and the IEEE Third Millennium Medal. From the IEEE Signal Processing Society he has been honored with the Education Award, the Society Award, the Technical Achievement Award and the Senior Award. He has also received a number of awards at MIT for excellence in teaching, including the Bose Award, the Everett Moore Baker Award, and several awards for outstanding advising and mentoring.

Analysis and Realization of Amplitude Sampling

Pablo Martínez-Nuevo, Hsin-Yu Lai, *Student Member, IEEE,* and Alan V. Oppenheim, *Life Fellow, IEEE*

Abstract

The theoretical basis for conventional acquisition of bandlimited signals typically relies on uniform time sampling and assumes infinite-precision amplitude values. In this paper, we explore signal representation and recovery based on uniform amplitude sampling with assumed infinite precision timing information. The approach is based on the concept of reversibly transforming a nonmonotonic input signal into a monotonic one which is then uniformly sampled in amplitude. In effect, the monotonic function is then represented by the times at which the signal crosses a predefined and equally-spaced set of amplitude values. We refer to this technique as amplitude sampling. When the transformation into a monotonic function is based on ramp addition, for practical purposes, the approach can be implemented by applying a one-level level-crossing detector to the result of adding an appropriate sawtooth-like waveform to the source signal. The time sequence generated by the level crossings can be interpreted alternatively as nonuniform time sampling of the original source signal or uniform amplitude sampling of the monotonic function to which it is transformed. We derive duality and frequency-domain properties for the functions involved in the transformation. Iterative algorithms are proposed and implemented for recovery of the original source signal and compared with nonuniform time sampling reconstruction methods of the original source signal. As indicated in the simulations, the proposed iterative amplitude-sampling algorithm achieves a faster convergence rate than reconstruction based on nonuniform sampling.

This work was supported in part by Texas Instruments Leadership University Program. The work of P. Martínez-Nuevo was also supported in part by Fundación Rafael del Pino, Madrid, Spain. The work of H. Lai was also supported in part by the Jacobs Fellowship and the Siebel Fellowship.

P. Martínez-Nuevo was with the Department of Electrical Engineering and Computer Science, Massachusetts Institute of Technology. He is now with the research department at Bang&Olufsen, 7600 Struer, Denmark (e-mail: pmnuevo@alum.mit.edu).

H. Lai and A. V. Oppenheim are with the Department of Electrical Engineering and Computer Science, Massachusetts Institute of Technology, Cambridge MA 02139 USA (e-mail: hsinyul@mit.edu; avo@mit.edu).

Manuscript received April 19, 2005; revised August 26, 2015.

The performance can also be improved by appropriate choice of the parameters while maintaining the same sampling density.

Index Terms

Sampling theory, level-crossing sampling, nonuniform sampling and reconstruction, iterative algorithms.

I. Introduction

The theoretical foundation of conventional time sampling typically relies on the sampling theorem for bandlimited signals [1]–[3], which states that bandlimited signals can be perfectly represented by infinite-precision amplitude values taken at equally-spaced time instants appropriately separated. In this paper, we propose signal representation based on equally-spaced amplitude samples with infinite-precision timing information.

Signal representation based on discrete amplitudes and continuous time has previously been studied and utilized in a number of context. In [4] signal representation consists of the real and complex zeros of a bandlimited signal. Logan's theorem [5] characterizes a subclass of bandpass signals that can be completely represented, up to a scaling factor, by their zero crossings. Practical algorithms for recovery from zero crossings of periodic signals in this class have been proposed in [6]. Arbitrary bandlimited signals can also be implicitly described by the zero crossings of a function resulting from an invertible transformation [7]–[9]—for example, the addition of a sinewave [10, Theorem 1]. In principle, interpolation is possible through Hadamard's factorization [11, Chapter 5] although there are more efficient techniques in terms of convergence rate [12]–[15]. Zero-crossings have also been studied in relation to wavelet transforms [16]. In this case, stable reconstruction can be achieved by including additional information about the original signal.

The extension from zero crossings to multiple levels, in the context of data compression, was investigated in [17]. In that work, a sample is generated whenever the source signal crosses a predefined set of threshold levels. The time instants of the crossings and the level-crossings directions were utilized to represent the signal although time was still quantized due to practical considerations. A practical continuous-time version of level-crossing sampling was later proposed in [18]. Asynchronous delta modulation [19] is, also, in some sense, a precursor of level-crossing sampling since it generates a positive or negative pulse at time instants when the change in signal amplitude surpasses a fixed quantity.

The focus of previous work on level-crossing sampling and reconstruction has typically been approximate reconstruction and implementational simplicity. For example, recovery is often performed through

a zero- or first-order hold, possibly in combination with low-pass filtering [20], [21]. Although there exist elaborate reconstruction techniques for multidimensional signals [22], [23], practical and accurate signal reconstruction techniques for generalized level-crossing sampling in one dimension are still under-explored.

In this paper, we explore the concept of amplitude sampling with the signal represented by the time sequence of equally-spaced level crossings. In principle, if a signal were monotonic, then the crossings of equally-spaced amplitude levels would generate an ordered time sequence $\{t_n\}$ which could be considered as a representation of the signal. In effect, under appropriate conditions, this corresponds to uniform sampling in amplitude with the signal information contained in the time sequence $\{t_n\}$. Nonmonotonic signals can be reversibly transformed into monotonic ones which are then uniformly sampled in amplitude. We refer to this technique as amplitude sampling. As discussed in section II, when the reversible transformation consists of adding a ramp with appropriate slope, a more practical implementation to generate the identical ordered time sequence $\{t_n\}$ is that shown in Fig. 1. As shown in II the time sequence generated by the system in Fig. 1 and that obtained by uniform amplitude sampling after ramp addition are identical. For conceptual simplicity in the analysis in this paper, we utilize the interpretation of the time sequence $\{t_n\}$ as derived from uniform amplitude sampling of the monotonic function obtained by ramp addition.

In sections III, IV, and V we derive duality as well as time- and frequency-domain properties relating the functions present in the transformation. The structure of these functions suggest an iterative reconstruction algorithm for numerical recovery of the source signal from the amplitude samples. This algorithm is discussed in Section VI with simulations and comparisons with reconstruction based on the nonuniform time samples.

II. Principle of Amplitude Sampling

Consider first the process represented by the block diagram depicted in Fig. 1. The level detector produces an impulse at times at which the input signal reaches the value Δ. For ease of illustration, assume the ramp-segment generator initiates a ramp with slope $\alpha > 0$ that abruptly shifts down by Δ in amplitude whenever an impulse arrives. Assume α is chosen such that $\tilde{g}(t)$ is monotonic in each interval between successive impulses.

Fig. 2 shows an example of the signals involved in the process. By construction, the ramp segments of the function $r(t)$ present the same slope. This manifests itself in the presence of an continuous ramp of slope α separated by multiples of Δ for each corresponding segment. Consequently, the function $\tilde{g}(t)$, which is the addition of these segments and the input signal $f(t)$, presents the same characteristic with

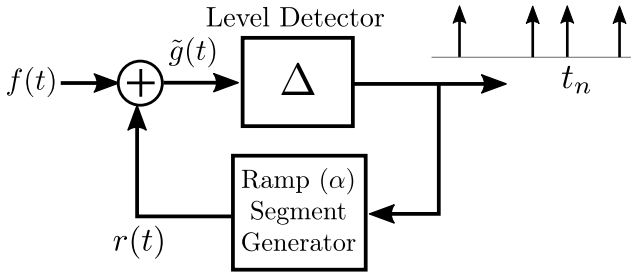

Fig. 1. Equivalent representation of the amplitude sampling process.

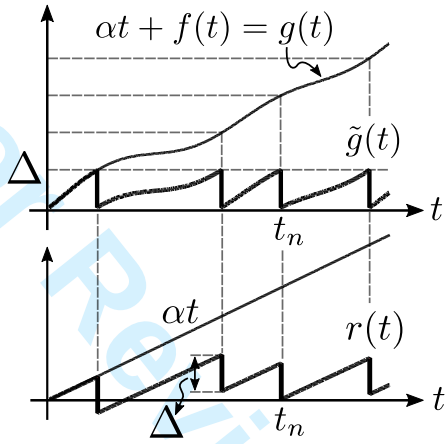

Fig. 2. Illustration of the different waveforms involved in the system shown in Fig. 1.

respect to $g(t) = \alpha t + f(t)$. In fact, the time instants at which the impulses are generated correspond precisely to the level-crossing instants of $g(t)$ for amplitude thresholds placed at multiples of Δ. Moreover, the function $g(t)$, assuming appropriate regularity conditions, has an inverse function $t(g)$ which is effectively sampled uniformly in the amplitude domain with samples corresponding to these time instants. Therefore, the sampling process of Fig. 1 can be interpreted as uniformly sampling the function $t(g)$. In principle, it is possible to generalize this this concept by considering any transformation that generates a monotonic function $g(t)$.

Amplitude sampling and reconstruction as developed in this paper is then based on the principle of reversibly representing and then sampling a time function $g(t)$ in the form $t(g)$ and then sampling in g. This requires that $g(t)$ be monotonic which means that if the source signal is nonmonotonic, it must first be reversibly transformed into a strictly monotonic function through a transformation ϕ. As illustrated in Fig. 3, the resulting function $\phi(f(t))$ is then uniformly sampled. The time instants $\{t_n\}$ at which $\phi(f(t))$ crosses the predefined set of amplitude values $\{n\Delta\}$ implicitly represents the source

signal, i.e. $\phi(f(t_n)) = n\Delta$ where $\Delta > 0$ is the separation between consecutive levels. Each of the time instants is paired exactly with one amplitude level. Thus, there exists a one-to-one correspondence between amplitude values and time instants. The sequence of time instants together with knowledge of Δ is sufficient information to describe the sampling process.

Amplitude sampling corresponds to signal-dependent nonuniform time sampling with the sampling density dependent on the source signal and the choice of the transformation ϕ.

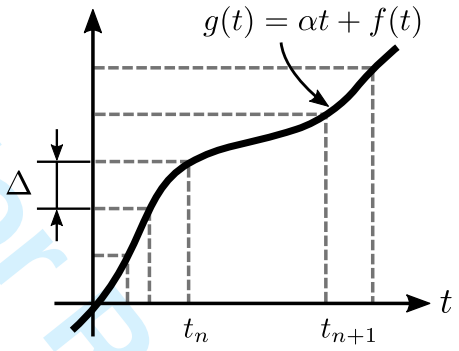

Fig. 3. Principle of amplitude sampling based on a transformation ϕ of the source signal f resulting in a monotonic function $\phi(f(t))$.

III. Transformation by Ramp Addition

There exist a myriad of transformations ϕ that can potentially generate a monotonic function from a given f. Among the simplest is the addition of a ramp with a sufficiently large slope. Suppose the original signal f is continuous, and it is possible to construct the strictly monotonic function $g(t) = \alpha t + f(t)$ for some $\alpha \in \mathbb{R}$. Then, the sampling process consists of the sequence of time instants $\{t_n\}$ satisfying $g(t_n) = \alpha t_n + f(t_n) = n\Delta$ for some $\Delta > 0$.

As indicated earlier, for analysis purposes in this paper, it is convenient to interpret the time sequence $\{t_n\}$ as resulting from sampling uniformly in amplitude the monotonic function $u = g(t) = \alpha t + f(t)$. In the context of this transformation, there exists an inverse function $g^{-1}(u)$ that we choose to express in the form $g^{-1}(u) = u/\alpha + h(u)$ for some amplitude-time function h. This interpretation suggests that this transformation can also be viewed as a mapping from f to the associated function h.

A. Mapping between f and h

The addition of a ramp represents a mapping, parametrized by the slope of the ramp, between the original signal and the function h. We denote this mapping by M_α, i.e. $M_\alpha f = h$ which can be viewed

as the addition of the ramp to obtain the monotonic function g and, after inverting g, subtracting the ramp u/α to obtain h. The reverse procedure to recover f from h consists of adding a ramp of slope u/α to h and utilizing the invertibility of g^{-1} as well as the correspondence between g and f. This inverse mapping is denoted by $M_{\alpha^{-1}}$ and satisfies $M_{\alpha^{-1}}h = f$. Fig. 4 illustrates the one-to-one correspondence between f and h. These mappings are also summarized in equation form as [24]

$$\begin{aligned} f(t) &= -\alpha h(f(t) + \alpha t) \\ h(u) &= -\frac{1}{\alpha} f(h(u) + \frac{u}{\alpha}). \end{aligned} \tag{1}$$

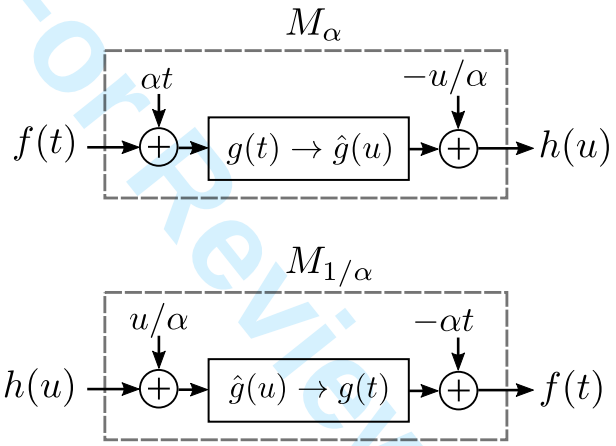

Fig. 4. Illustration of the invertibility of the transformation between f and h when $g(t) = \alpha t + f(t)$ and $g^{-1}(u) = u/\alpha + h(u)$.

As is evident from Fig. 4 and (1) there is a duality between M_α and its inverse. It is possible to interpret (1) as a signal-dependent warping operation that obtains f from h and vice versa. The addition of a ramp in amplitude sampling also generates an underlying mapping, dependent on f or h, between time t and amplitude u. Both mappings can be easily seen from (1) in its matrix form and the corresponding inverse matrix:

$$\begin{pmatrix} f(t) \\ t \end{pmatrix} = \begin{pmatrix} -\alpha & 0 \\ 1 & 1/\alpha \end{pmatrix} \begin{pmatrix} h(u) \\ u \end{pmatrix} \tag{2}$$

$$\begin{pmatrix} h(u) \\ u \end{pmatrix} = \begin{pmatrix} -1/\alpha & 0 \\ 1 & \alpha \end{pmatrix} \begin{pmatrix} f(t) \\ t \end{pmatrix}. \tag{3}$$

The duality implies that any properties of h inherited by assumptions made on f hold for f if the same assumptions are instead imposed on h.

B. The Sampling Process

Amplitude sampling produces a sequence of time instants corresponding to $n\Delta = g(t_n) = \alpha t_n + f(t_n)$ where $\Delta > 0$. In similar fashion, the inverse function $g^{-1}(u)$ and h are both uniformly sampled in amplitude, i.e.

$$g^{-1}(n\Delta) = n\Delta/\alpha + h(n\Delta) \tag{4}$$

and

$$h(n\Delta) = t_n - n\Delta/\alpha. \tag{5}$$

C. Sampling Density

As noted earlier, amplitude sampling in the form presented here can be viewed as equivalent to nonuniform time sampling. In this setting, stable reconstruction algorithms typically impose conditions on the sequence of sampling instants as for example the Landau rate [25] for bandlimited signals. In order to gain insight into the time-sampling density inherent in our amplitude-sampling process, assume the source signal f has a bounded derivative, i.e. $|f'(t)| \leq B$ for some $B > 0$ and that $|\alpha| > B$ so that the function $g(t) = \alpha t + f(t)$ is strictly monotonic. Then the time between successive samples satisfies the inequality

$$\frac{\Delta}{|\alpha| + B} \leq |t_{n+1} - t_n| \leq \frac{\Delta}{|\alpha| - B}. \tag{6}$$

where $\Delta > 0$ is the separation between consecutive amplitude levels.

The bounds in (6) are consistent with intuition. For example, assume that α is positive. The derivative of g is bounded by $\alpha + B$ which provides the minimum attainable time separation between crossings. Similarly, the maximum separation is essentially limited by $\alpha - B$. The quantization step Δ represents the change in amplitude necessary to produce a sample. Additionally, when α achieves sufficiently large values, the bounds for time separation become closer, or equivalently, the time sequence becomes more uniform. We can observe this effect in (6) where amplitude is approximately a scaled version of the time axis.

D. Iterative Algorithm for the Realization of M_α

In this section, we propose an iterative algorithm for the implementation of M_α to generate $h(u)$ from $f(t)$. By duality, an equivalent algorithm can be used for the implemention of $M_{\alpha^{-1}}$ to generate $f(t)$

from $h(u)$. For ease of illustration, we consider a modified version of the transformation M_α defined in (7) which we denote by $\tilde{M}_\alpha$:

$$\begin{aligned} f(t) &= \tilde{h}(\frac{1}{\alpha}f(t) + t) \\ \tilde{h}(u) &= f(-\frac{1}{\alpha}\tilde{h}(u) + u). \end{aligned} \tag{7}$$

Equations (7) form the basis for the iterative algorithm formalized in the following theorem.

Theorem 1: Let the function f be Lipschitz continuous with constant $< \alpha$ and suppose that $\sup_{t\in\mathbb{R}} |f(t)| \leq A$. Then, the function $\tilde{h}(u) = (\tilde{M}_\alpha f)(u)$ for $u \in \mathbb{R}$ can be obtained by the iteration

$$\tilde{h}_{n+1}(u) = f(u - \frac{1}{\alpha}\tilde{h}_n(u)) \tag{8}$$

for $n \geq 0$ where $\tilde{h}_0(u) = f(u)$ and $\tilde{h}_n(u) \to \tilde{h}(u)$ as $n \to \infty$.

The detailed proof is carried out in Appendix A.

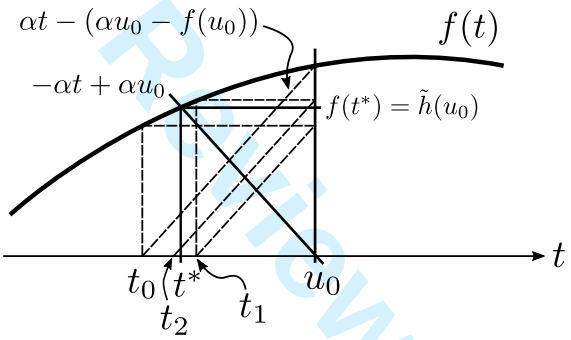

Fig. 5. Illustration of the iteration described in Theorem 1 with the initialization $t_0 = u_0$.

As used in the preceding, the value of $\tilde{h}(u_0)$ can be obtained from the first equality in (7). In particular, $\tilde{h}(u_0) = f(t^*)$ where t^* is the value that satisfies $u_0 = t^* + f(t^*)/\alpha$. The solution is unique since the slope of the ramp, in absolute value, is always greater than the maximum value of the derivative of f. As shown in Fig. 5, t_0 is the time instant at which the ramp $\alpha t_0 - \alpha t$ intersects the function $f(t)$. In the same way, the value of the $(n+1)$-th iteration can be viewed as the solution of $\alpha t - (\alpha u_0 - f(t_n)) = 0$. In other words, we iteratively construct a straight line passing through the point $(u_0, f(t_n))$. The intersection with the horizontal axis then corresponds to the value of t_{n+1}.

IV. Spectral Properties

Assumptions made on the source signal f are naturally reflected in the structure of h. In this section, we assume that f is a bandlimited function and derive properties regarding the spectral content of the

amplitude-time function h. The duality between f and $h = M_\alpha f$ implies that similar conclusions can be made about f when h is assumed to be bandlimited.

As an example to motivate the discussion, consider the bandlimited input signal $f(t) = \mathrm{sinc}(t)$ to produce $h = M_\alpha f$ where α is assumed to be positive and large enough so that $g(t) = f(t) + \alpha t$ is strictly monotonic. Fig. 6 depicts both functions f and h. Note that h presents shear-like behavior relative to to the shape of f. This effect is caused by the subtraction of a ramp from the parts of g where its derivative is small. Since, the derivative of g^{-1} is the reciprocal of g, these regions also correspond to large values of the derivative of h. This structure may entail the presence of relevant energy at high frequencies. In particular, we could expect that the frequency-domain characteristics of h are roughly controlled by the difference $\alpha - B$ for $|f'(t)| \leq B$.

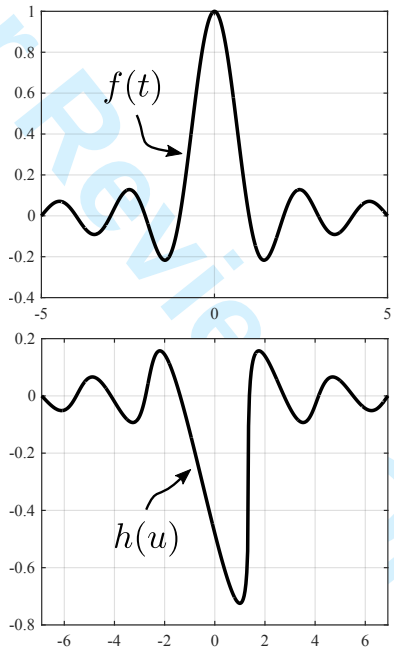

Fig. 6. Example of the transformation in amplitude sampling where $f(t) = \mathrm{sinc}(t)$, $\alpha = 1.38$, and $h = M_\alpha f$.

In exploring the spectral content of h we assume that f is bandlimited to σ rad/s with $\sigma > 0$ and bounded in amplitude, i.e. $|f(t)| < A$ for some A. We further assume that the decay of $f(t)$ for t real satisfies $|f(t)| \leq A/(1+t^2)$. In principle, the extension to square-integrable functions is straightforward. With our assumptions on f, Bernstein's inequality [26] provides the bound $|f'(t)| \leq A\sigma$ for all $t \in \mathbb{R}$. This bound gurantees that the function u defined as

$$u = g(t) = \alpha t + f(t). \tag{9}$$

will be strictly monotonic whenever $|\alpha| > A\sigma$. The function h is then given by $h(u) = g^{-1}(u) - u/\alpha$. From Theorem 2 below it follows that the decay of the Fourier transform of h, denoted by $\hat{h}(\xi)$ for ξ in Hz, satisfies $\hat{h}(\xi) = \mathcal{O}(e^{-2\pi|\xi|b})$ as $\xi \to \infty$ where $b > 0$ is determined by the difference $|\alpha| - A\sigma$.

Theorem 2: Let $f(t) : \mathbb{R} \to \mathbb{R}$ be a continuous function bandlimited to $\sigma > 0$ rad/s. Assume further that $|f(t)| \leq A/(1 + t^2)$ for all $t \in \mathbb{R}$ and some $A > 0$. Construct the function

$$u = g(t) = \alpha t + f(t) \tag{10}$$

for $|\alpha| > A\sigma$. Then, there exists $g^{-1}(u)$ for all $u \in \mathbb{R}$ and a constant $C > 0$ such that the Fourier transform of $h(u) = g^{-1}(t) - u/\alpha$ satisfies $|\hat{h}(\xi)| \leq Ce^{-2\pi|\xi|b}$ for any $0 \leq b < a$ such that

$$a = \frac{|\alpha|}{\sigma} \log\left(\frac{|\alpha|}{A\sigma}\right) - \frac{|\alpha| - A\sigma}{\sigma}. \tag{11}$$

and $\xi \in \mathbb{R}$.

The detailed proof is carried out in Appendix B.

As anticipated, the rate of decay of the Fourier transform at infinity depends on $|\alpha| - A\sigma$. The difference is logarithmic in the first term and linear in the second one. The larger the difference the faster the decay at infinity. Note that $a > 0$ always holds since $|\alpha| > A\sigma$. Assuming $\alpha > 0$, this difference is precisely impacting the highest slope portions in h, or, equivalently, the regions in which f' is smallest. The underlying reason being that the derivative of g^{-1} is the reciprocal of g, i.e. $(g^{-1}(u))' = 1/g'(g^{-1}(u))$ for all $u \in \mathbb{R}$. Informally, it is the tilted regions in the shape of h are responsible, to some extent, for the high-frequency content.

It should be emphasized that any bandlimited function will naturally be in the class of signals whose spectrum exhibits at least exponential decay at infinity. However, Theorem 3 stated below asserts that f and h cannot be simultaneously bandlimited. The precise statement in the description of the theorem guarantees this property with the possible exception of, at most, one value of α. For practical purposes, we can ignore this isolated case.

Theorem 3: Under the conditions of Theorem 2 and unless f is constant, the function $h(u)$ is nonbandlimited for every $\alpha > A\sigma$ with at most one exception.

The detailed proof is carried out in Appendix C.

In the singular case, in which f is a constant, it can be shown through the constructive process of M_α by ramp addition that h is constant as well, specifically, for $f = A$, then $h = -A/\alpha$. From another point of view, according to (1), the function f results, in general, from h with a nonlinear warping of the independent variable. When either of the two functions is constant, the warping is affine. Therefore, in this case, the bandlimited property is preserved [27]. In our context the conclusion follows directly from (1) that if either f or h is constant, the other must be also.

More generally, if $|\alpha|$ increases significantly, the warping function becomes approximately linear since $f(t)$ is negligible compared to αt, i.e. $f(t) \approx -\alpha h(\alpha t)$. This is consistent with (11) where an increase of $|\alpha|$ produces a faster decay at infinity of $\hat{h}$.

V. Time-Domain Decay Properties

In some sense, h inherits characteristics of f since it is a "time-warped" version of f. In this section, we show the connections between the properties of f and h in the time domain with the relationship between f and h as specified in (1) which explicitly requires that the slope of the ramp added to f and the slope of the ramp subtracted to obtain h be exact inverses. Intuitively, it is not surprising that the function h should present decay properties similar to those of f once the unbounded growth of the ramp component has been subtracted. In particular, it is stated in [28, Chapter 2, Proposition 1] that when the slopes of the two ramps as inverses, the decay of h will match that of f. Otherwise h does not decay appropriately on the real line.

The transformation M_α also has an impact on the L^p norms of the respective functions with the parameter α playing a crucial role. It can be shown that the decay on the real line of both functions is related by [28, Chapter 2, Proposition 3]

$$||h||_p = \frac{1}{\alpha^{1-\frac{1}{p}}}||f||_p, \ p \in [1, \infty]. \tag{12}$$

Not only does h belong to $L^p(\mathbb{R})$ if f does, but their respective norms are also related by a scaling factor which is precisely α. Indeed, for very large values of $|\alpha|$, the ramp approaches the vertical axis, thus reducing the range of h and decreasing the norm.

In terms of a sense of distance, let f_1 and f_2 generate h_1 and h_2 respectively. The transformation M_α preserves the L^1 distance [28, Chapter 2, Proposition 4], i.e.

$$||h_1 - h_2||_1 = ||f_1 - f_2||_1. \tag{13}$$

By duality, these properties hold irrespective of the role of each function as an input or output.

VI. Reconstruction in Amplitude Sampling

Amplitude sampling can be interpreted as signal-dependent nonuniform time sampling of the source signal f based on uniform time sampling of the associated amplitude-time function h. If f is bandlimited, then as was shown in Section IV h is not bandlimited and consequently cannot be exactly reconstructed through bandlimited interpolation. Our reconstruction approach begins by initially using sinc interpolation as an approximation. This is then extended to an iterative algorithm that achieves accurate recovery. Throughout this entire section, we assume that the source signal f is bandlimited to σ rad/s, and $|f(t)| \leq A/(1+t^2)$ for $A > 0$ and all $t \in \mathbb{R}$.

A. Bandlimited Interpolation Algorithm (BIA)

The approximate reconstruction of f based on sinc interpolation of h is depicted in Fig. 7. From this approximation to h an approximation to f is generated through $M_{\alpha^{-1}}$ which is then lowpass filtered since f is assumed to be bandlimited. In particular, the D/C system is defined by the relationship

$$h_\Delta(u) = \sum_{k\in\mathbb{Z}} h(k\Delta)\mathrm{sinc}(u/\Delta - k). \tag{14}$$

Note that the samples of h are related to $\{t_n\}$ as $h(n\Delta) = t_n - n\Delta/\alpha$, $n \in \mathbb{Z}$. At this stage the approximation can be quantified as [28, Chapter 3, Proposition 6]

$$||h - h_\Delta||_\infty \leq \frac{C'}{a} e^{-\pi \frac{a}{\Delta}}. \tag{15}$$

The error in (15) is then controlled both by the difference $|\alpha| - A\sigma$ and the quantization step size Δ. As already discussed, increasing the difference $|\alpha| - A\sigma$ produces, in some sense, a function h with a faster high-frequency spectral decay and therefore one that is more approximately bandlimited. Thus, we would expect that the performance of the approximation can be improved by increasing this difference.

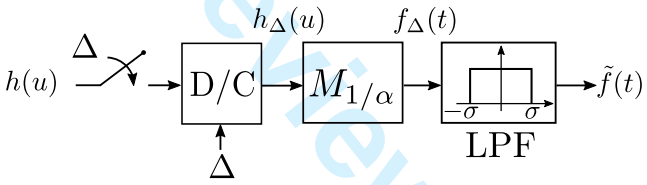

Fig. 7. Approximate reconstruction procedure for a bandlimited source signal f such that $h = M_\alpha f$. The block D/C is a discrete-to-continuous operation involving sinc interpolation with period Δ.

B. Iterative Amplitude Sampling Reconstruction (IASR)

The bandlimited interpolation algorithm (BIA) forms the basis for an iterative algorithm which we refer to as the Iterative Amplitude Sampling Reconstruction (IASR) algorithm illustrated in Fig. 8. Note that if the initialization satisfies $h_0(u) \equiv 0$ and $f_0(t) \equiv 0$, the first iteration corresponds precisely to BIA, i.e. $f_1(t) = \tilde{f}(t)$. Similar to the approximate bandlimited recovery, the emphasis is placed on the reconstruction of h from its nonuniform amplitude samples and then imposing the bandlimited constraint on the successive approximations to f with the objective of iteratively reducing the error $||e_k(t)||_2$.

C. Simulation Results

In all of the simulations in this section, the source signal f is chosen as white noise bandlimited to σ rad/s and bounded by $A > 0$. The quantization step size Δ and the parameter α are chosen so that the

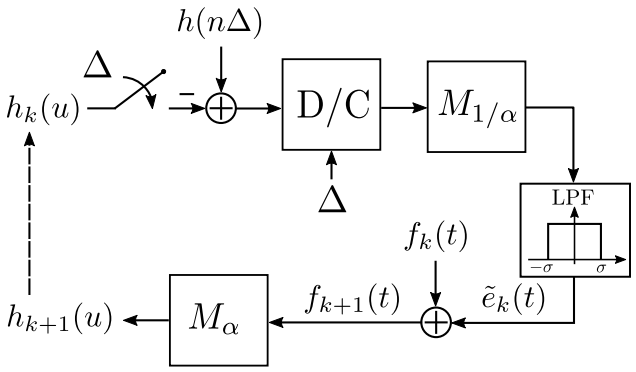

Fig. 8. Block diagram representation of the iterative amplitude sampling reconstruction (IASR) algorithm.

sampling density is greater or equal than the Landau rate [25], which, in our case, is given by π/σ. We choose as a measure of approximation error the signal-to-error ratio (SER) given by

$$\text{SER} = 10\log_{10}\left(\frac{||f_k||_2^2}{||f - f_k|_2^2}\right) \tag{16}$$

where f_k is the k-th iteration.

Since amplitude sampling also implies nonuniform time sampling on the source signal f, we also directly apply a nonuniform reconstruction algorithm to recover f. Specifically, we compare IASR to the Voronoi method developed in [29, Theorem 8.13]. Based on the bounds in (6) for the time instants, it is straightforward to see that the sampling instants in an amplitude sampling setting satisfy the requirements of the Voronoi method for an appropriate choice of the parameters. In particular, it can be shown that it is sufficient that

$$\frac{\Delta}{|\alpha| - A\sigma} > \frac{\pi}{\sigma}. \tag{17}$$

In initializing both algorithms, the 0-th iteration in both IASR and the Voronoi method is assumed to be zero.

In Fig. 9, we have modified individually the parameters α or Δ. In reducing the value of the quantization step size Δ, the transformed function $\alpha t + f(t)$ will clearly cross more amplitude levels per unit of time. Similarly, when the slope of the ramp added to f is increased in absolute value, it also causes an increase in the level-crossing density. Thus, both effects result in an increase of the sampling density, and, as shown in the figure, the rate of convergence improves. However, it can be observed that the rate of convergence is faster in the IASR case. The first iteration in IASR achieves a better approximation than the Voronoi method although the rate of convergence appears to be highly insensitive to this change of parameters. On the other hand, the Voronoi method is significantly impacted by the change in sampling density. Moreover, it requires several iterations until it obtains the same approximation performance as the first

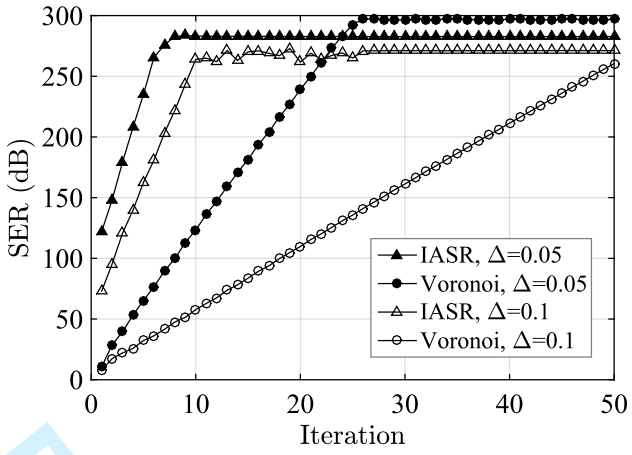

(a)

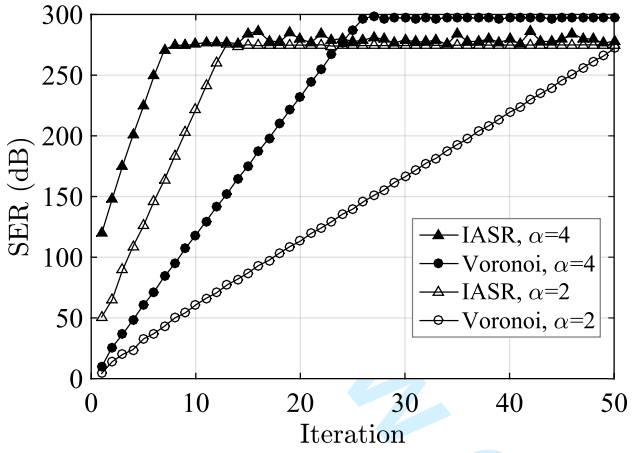

(b)

Fig. 9. Performance comparison between IASR, AWM, and BIA, for a broadband input signal bandlimited and bounded; (a) Δ is changed while α is fixed; (b) α is changed while Δ is fixed.

iteration in IASR. As shown in Fig. 10 the same conclusions hold if we increase the oversampling ratio by considering signals with smaller bandwidths and, at the same time, keeping α and Δ fixed.

Thus far, we have focused on modifying the sampling density. Additionally, due to the structure of the sampling process in amplitude sampling, it is also possible to keep the sampling density fixed while changing both α and Δ accordingly. The rate of convergence in the Voronoi method is determined by the maximal separation between consecutive sampling instants. With constant sampling density, the performance of the Voronoi method does not change, as shown in Fig. 11. However, IASR presents an improvement in the rate of convergence. This is not surprising since the difference $|\alpha| - A\sigma$ has increased,

which likely results in a better approximation of the sinc interpolation in IASR.

When the input signal is highly oversampled, we have empirically observed that the Voronoi method has a faster rate of convergence. Nevertheless, when the sampling instants become increasingly sparse approaching the Landau rate, IASR performs significantly better.

In summary, overall, IASR appears to have better performance than the Voronoi method in terms of speed of convergence when the sampling density approaches the Landau rate. Changes in the sampling density have a higher impact on the convergence in the Voronoi method than in IASR. Moreover, IASR performance can also be improved by increasing the difference $|\alpha| - A\sigma$ while keeping the sampling density invariant. In [24], a scaling of the input signal also produces an increase in the speed of convergence. This performance improvement of IASR over the Voronoi method may be due to the characteristics of the sampling instants. Specifically the sampling instants in IASR inherently incorporate the amplitude sampling structure and therefore contain more information initially than more general nonuniform sampling would. In some sense, this may suggest that IASR is designed to more effectively exploit the structure of this particular sampling process which implicitly is signal dependent and consequently signal information is implicitly embedded in both the sampling times and the sample values.

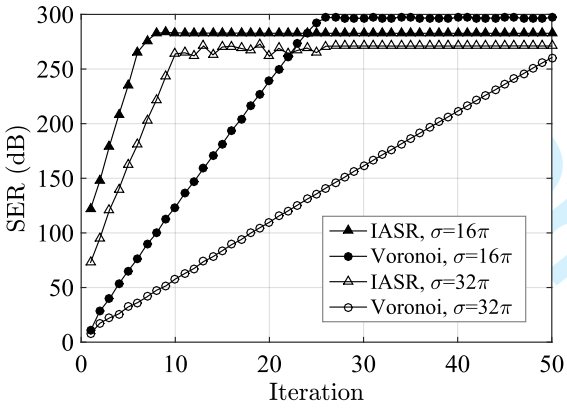

Fig. 10. Performance comparison between IASR and the Voronoi method when the bandwidth σ is changed, and α and Δ are fixed.

VII. Conclusion

Amplitude sampling represents a signal with equally-spaced amplitude values and infinite-precision timing information by reversibly transforming the source signal. This transformation provides the perspective of viewing amplitude sampling as uniform sampling of an associated amplitude-time function

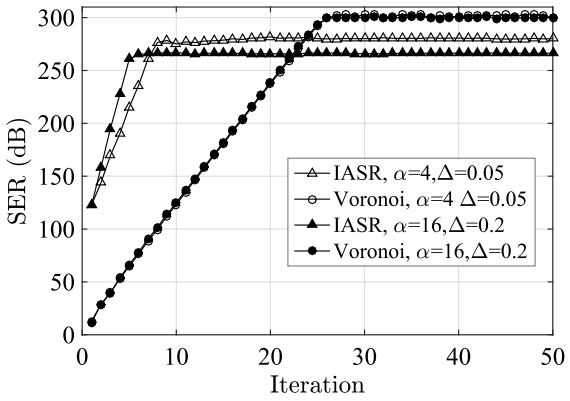

Fig. 11. Performance comparison between IASR and the Voronoi method when the sampling density is fixed and α and Δ are changed.

or equivalently as nonuniform time sampling of the source signal. The properties of both functions are connected by a duality relationship. Similarly, an iterative algorithm for recovery was proposed and evaluated that exploits the particular characteristics of the sampling instants in amplitude sampling. For the amplitude sampling structure this algorithm outperforms the use of more general nonuniform reconstruction algorithms.

APPENDIX A
PROOF OF THEOREM 1

According to (7), obtaining $\tilde{h}(u_0)$ for some fixed $u_0 \in \mathbb{R}$ is equivalent to finding some $t^* \in \mathbb{R}$ such that $u_0 = t^* + f(t^*)/\alpha$ since $\tilde{h}(u_0) = f(t^*)$. Therefore, we have to find the roots of

$$t = u_0 - \frac{1}{\alpha} f(t) \triangleq v_{u_0}(t) \tag{18}$$

for $t \in \mathbb{R}$. It is easy to see that $v_{u_0}(t)$ is Lipschitz continuous for some constant $K < 1$. Furthermore, there always exists some $\epsilon \geq A/\alpha$ such that $v_{u_o} : I \to I$ where $I = [u_0 - \epsilon, u_0 + \epsilon]$. Thus, the Banach fixed-point theorem [30] guarantees the uniqueness and existence of a solution. Moreover, it ensures convergence with the following bounds for the error

$$|t_{n+1} - t^*| \leq K|t_n - t^*| \tag{19}$$

for $n \geq 0$ where $t_0 \in I$ and $t_{n+1} = v_{u_0}(t_n)$. Then, the iteration can be equivalently expressed in terms of the functional composition form as

$$\tilde{h}_{n+1}(u_0) = f(u_0 - \frac{1}{\alpha}\tilde{h}_n(u_0)). \tag{20}$$

Since u_0 was chosen arbitrarily, the same conclusions hold for any $u_0 \in \mathbb{R}$. □

APPENDIX B
PROOF OF THEOREM 2

We first introduce several results that will become useful in the proof of the theorem. Define the open disk in the complex plane centered at z_o and of radius r as

$$D_r(z_o) = \{z \in \mathbb{C} : |z - z_o| < R\} \tag{21}$$

and use $\overline{D}_r(z_o)$ for its closure.

Lemma 1: Let f be a holomorphic function in some region Ω with power series $f(z) = \sum_{n=0}^{\infty} a_n(z - z_o)^n$ at $z_o \in \Omega$. Consider a disk of radius R centered at z_o such that Ω contains the disk and its closure. If $a_1 \neq 0$ and

$$|a_1| > \sum_{n=2}^{\infty} |a_n| n R^{n-1}, \tag{22}$$

then f is injective in any open disk of radius $r \leq R$.

Proof 1: Without loss of generality assume $z_o = 0$, thus the power series expansion of f around the origin is given by $f(z) = \sum_{n=0}^{\infty} a_n z^n$ for all $z \in \Omega$. Take $z_1, z_2 \in \overline{D}_R(0) \subset \Omega$ such that $z_1 \neq z_2$ and recall that for any $z, w \in \mathbb{C}$ the following identity holds

$$(z^n - w^n) = (z - w)(z^{n-1} + z^{n-2}w + \ldots + zw^{n-2} + w^{n-1}). \tag{23}$$

We can write

$$\begin{aligned}
\left|\frac{f(z_2) - f(z_1)}{z_2 - z_1}\right| &= \left|a_1 + \sum_{n=2}^{\infty} a_n \frac{z_2^n - z_1^n}{z_2 - z_1}\right| \\
&= \Big|a_1 + \sum_{n=2}^{\infty} a_n (z_2^{n-1} + z_2^{n-2} z_1 + \ldots \\
&\qquad \ldots + z_2 z_1^{n-2} + z_1^{n-1})\Big| \\
&\geq |a_1| - \sum_{n=2}^{\infty} |a_n| n R^{n-1}.
\end{aligned}$$

where the last inequality follows from the reverse triangle inequality and the fact that $|z_1|, |z_2| \leq R$. Thus, if $|a_1| - \sum_{n=2}^{\infty} |a_n| n R^{n-1} > 0$, then $f(z_2) - f(z_1) \neq 0$ and $f(z)$ is injective in $D_r(z_o)$ for any $r \leq R$. □

Proposition 1: Let $f : U \to V$ be a bijective continuous function. Consider a set Ω such that its closure $\overline{\Omega}$ is strictly contained in U, then $f(\partial\Omega) = \partial f(\Omega)$.

Proof 2: Consider $x \in \partial\Omega$, which is clearly a limit point of Ω. We know there exist a convergent sequence $x_n \to x$ for $n \geq 1$, where $x_n \in \Omega$. By continuity, we have that $f(x_n) \to f(x)$ is a convergent sequence in V. As f is a bijection from U to V, we have that $f(x_n) \neq f(x)$ for all $n \geq 1$, thus

$f(x) \in \overline{f(\Omega)}$. Moreover, $f(x) \neq f(x')$ for all $x' \in \Omega$, therefore $f(x) \in \partial f(\Omega)$ for all $x \in \partial\Omega$. It follows that $f(\partial\Omega) \subseteq \partial f(\Omega)$.

Now, we claim that for every $y \in \partial\Omega$ there exists an $x \in \partial\Omega$ such that $y = f(x)$. Imagine this is not true and there exists an $x_o \in U \setminus \partial\Omega$ such that $y_o = f(x_o)$. From our previous discussion, it is clear that x_o cannot be in Ω, then imagine $x_o \in U \setminus \overline{\Omega}$. Since f is continuous and bijective, we can choose a sufficiently small $\epsilon > 0$ such that $f^{-1}(D_\epsilon(y_o)) \subset D_\delta(x_o)$ and $D_\delta(x_o) \cap \overline{\Omega} = \emptyset$ for some $\delta > 0$. However, as y_o is a point in the boundary, it holds that $D_\epsilon(y_o) \cap f(\Omega) \neq \emptyset$. Thus, there exist an $x_1 \in \Omega$ such that $f(x_1) = y'$ for some $y' \in D_\epsilon(y_o)$. At the same time, there also exists an $x_2 \in f^{-1}(D_\epsilon(y_o))$ such that $f(x_2) = y'$, where $x_1 \neq x_2$. This contradicts the bijectivity assumption, thus $f(\partial\Omega) \supseteq \partial f(\Omega)$ which together with $f(\partial\Omega) \subseteq \partial f(\Omega)$ gives $f(\partial\Omega) = \partial f(\Omega)$. □

Proposition 2: Suppose $f(z)$ is an entire function of exponential type σ such that $|f(x)| \leq A/(1+x^2)$ for all $x \in \mathbb{R}$. Then, the following bound holds for all $z \in \mathbb{C}$

$$|f(z)| \leq \frac{Ae^{\sigma|y|}}{1+x^2}. \tag{24}$$

Proof 3: By assumption, we have that $|f(z)| \leq Ae^{\sigma|z|}$ for all $z \in \mathbb{C}$. Construct the function $F(z) = (1/A)(1+x^2)e^{i\sigma z}f(z)$, then F is bounded by 1 on the positive imaginary and positive real axis. If we consider the first quadrant $Q = \{z = x+iy : x > 0, y > 0\}$, it is clear that there exists constants $C, c > 0$ such that $|F(z)| \leq Ce^{c|z|}$ for $z \in Q$. We conclude by the Phragmén-Lindelöf theorem that $|F(z)| \leq 1$ for all z in Q. This implies that $|f(z)| \leq Ae^{\sigma y}/(1+x^2)$ for $z \in Q$. Using the same argument, one can show that the same is true in the second quadrant. For the third and fourth quadrants we use instead the function $F(z) = (1/A)(1+x^2)e^{-i\sigma z}f(z)$, which shows that (24) also holds for $y \leq 0$. □

The function f is of moderate decrease. By the Paley-Wiener theorem, its Fourier transform is then supported on $[-M, M]$. Thus, Bernstein's inequality implies that $|f'(x)| \leq \sigma A$. Now, we can split the proof of the theorem in three steps.

Step 1. We claim that the function $u = g(x) = \alpha x + f(x)$ admits a real analytic inverse function whenever $\alpha > \sigma A$. It is clear that $g(x)$ is analytic for all $x \in \mathbb{R}$ since it is the sum of two analytic functions on the whole real line. Moreover, $g(x)$ is a strictly increasing monotone function because $|f'(x)| \leq A\sigma$ and $\alpha > A\sigma$, which implies $g'(x) > 0$. The Real Analytic Inverse Function theorem guarantees that for a point x_o where $g'(x_o) \neq 0$, there exists a neighborhood J_o of x_o and a real analytic function g^{-1} defined on an open interval I_o containing $g(x_o)$ satisfying $(g^{-1} \circ g)(x) = x$ for $x \in J_o$ and $(g \circ g^{-1})(u) = u$ for $y \in I_o$. Since $g'(x) \neq 0$ for all real x, it is always possible for any given $x_1 \in \mathbb{R}$ to find an $x_2 \notin J_1$ such that $J_1 \cap J_2 \neq \emptyset$. Thus, by analytic continuation, we conclude that $g^{-1}(u)$ is analytic on the whole real line.

Step 2. We show that the function $g^{-1}(w)$ is analytic in a region containing the horizontal strip

$$S_a = \{w \in \mathbb{C} : |\mathrm{Im}(w)| < a, \\ \text{where } a = \frac{\alpha}{\sigma}\log\left(\frac{\alpha}{\sigma}\right) - \frac{\alpha-\sigma}{\sigma}\}. \tag{25}$$

The function $g(z) = \alpha z + f(z)$ is an entire function of exponential type σ and admits a power series expansion around $x \in \mathbb{R}$

$$g(z) = \alpha z + \sum_{n=0}^{\infty} \frac{f^{(n)}(x)}{n!}(z-x)^n \tag{26}$$

for all $z \in \mathbb{C}$. By Bernstein's inequality, the derivatives of f are bounded on the real line by $|f^{(n)}(x)| \leq A\sigma^n$. We now look for a region where $g(z)$ is injective. Using Lemma 1, $g(z)$ is injective in a disk of radius $R > 0$ whenever

$$|\alpha + f'(x)| > \frac{A}{R}\sum_{n=2}^{\infty} n\frac{(\sigma R)^n}{n!} = A\sigma(e^{R\sigma} - 1) \tag{27}$$

or, equivalently

$$R < \frac{1}{\sigma}\log\left(1 + \frac{|\alpha + f'(x)|}{A\sigma}\right). \tag{28}$$

The right-hand side of this expression is lower bounded by $(1/\sigma)\log(1 + (\alpha - A\sigma)/A\sigma) > 0$, since $|f'(x)| \leq A\sigma < \alpha$ for all $x \in \mathbb{R}$. Thus, it is always possible to choose a disk of positive radius satisfying this lower bound such that $g(z)$ is injective.

Let us fix an R satisfying this lower bound. Remember that holomorphic functions are open mappings, i.e. they map open sets to open sets. Thus, $g(z)$ maps an open disk of radius R to the open set $g(D_R(x))$. By continuity, $g(D_R(x))$ is also connected since $D_R(x)$ is connected. Therefore, the mapping $g(z) : D_R(x) \to g(D_R(x))$ represents a holomorphic bijection, thus its inverse is also holomorphic. Moreover, the inverse agrees with $g^{-1}(u)$ for real $u \in g(D_R(x))$. Thus, it represents the analytic continuation of $g^{-1}(u)$ on $u \in g(D_R(x))$. In fact, we can always choose a disk $D_R(x')$ such that $g(D_R(x)) \cap g(D_R(x')) \neq \emptyset$, where the inverse functions defined on their respective images take the same value in the intersection for real u. Again, by analytic continuation, we can analytically extend $g^{-1}(u)$ to $g(D_R(x)) \cup g(D_R(x'))$. Repeating this process for all real x, we obtain the analytic continuation of $g^{-1}(u)$ in the open set $\Omega = \cup_{x\in\mathbb{R}} g(D_R(x))$.

We want to find an $a > 0$ such that $S_a \subseteq \Omega$. Using Lemma 1, the boundary of the disk $\partial D_R(x)$ is mapped bijectively to $\partial g(D_R(x))$. Therefore, the largest radius ρ for a disk centered at $g(x)$ such that $D_\rho(g(x)) \subseteq g(D_R(x))$ for all $x \in \mathbb{R}$ is given by

$$\rho = \inf_{x\in\mathbb{R}} \sup_{|z-x|=R} \{|g(z) - g(x)| : \\ D_{|g(z)-g(x)|}(g(x)) \subseteq g(D_R(x))\}. \tag{29}$$

We can use the power series expansion of g around x to find a lower bound for ρ in the following manner

$$\begin{aligned} |g(z)-g(x)| &= |\alpha(z-x)+\sum_{n=1}^{\infty} a_n(z-x)^n| \\ &\geq \alpha R - \sum_{n=1}^{\infty} \frac{A\sigma^n}{n!} R^n = \alpha R - A(e^{R\sigma}-1). \end{aligned}$$

for $|z-x|=R$. The right-hand side of the last expression represents a strictly concave function of R, thus the maximum is achieved for

$$R = \frac{1}{\sigma}\log\left(\frac{\alpha}{A\sigma}\right) > 0 \tag{30}$$

which is positive as $\alpha > A\sigma$ and satisfies the upper bound in (28). Setting the value of R as in (30), we can write

$$|g(z)-g(x)| \geq \rho \geq \frac{\alpha}{\sigma}\log\left(\frac{\alpha}{A\sigma}\right) - \left(\frac{\alpha - A\sigma}{\sigma}\right) \tag{31}$$

for all $x \in \mathbb{R}$ and $|z-x|=R$. This implies that $S_a \subseteq \Omega$ for any a such that

$$a < \frac{\alpha}{\sigma}\log\left(\frac{\alpha}{A\sigma}\right) - \left(\frac{\alpha - A\sigma}{\sigma}\right). \tag{32}$$

Step 3. We show that $h(w)$ is of moderate decay on each horizontal line $|\mathrm{Im}(w)| < a$, uniformly in $|y| < a$. First, we note that since f is an entire function of exponential type σ and is of moderate decrease along the real line, by Proposition 2

$$|f(z)| \leq \frac{Ae^{\sigma|y|}}{1+x^2} \tag{33}$$

for all $z \in \mathbb{C}$. Let us now fix an R satisfying (30), then we have a bijection from $D_R(x')$ to $g(D_R(x'))$ for some $x' \in \mathbb{R}$. Therefore, $z = g^{-1}(w)$, where $w \in g(D_R(x))$ and $z \in D_R(x')$. Since $|y| < R$ for $z \in D_R(x')$, we also have $|f(z)| = |\alpha z - g(z)| \leq Ae^{\sigma R}/(1+x^2)$, or equivalently

$$|w - \alpha g^{-1}(w)| \leq \frac{Ae^{\sigma R}}{1+(g^{-1}(u))^2} \tag{34}$$

whenever $w \in g(D_R(x))$ and $z \in D_R(x')$. Using the reverse triangle inequality in the previous expression for real w, we can also obtain

$$|g^{-1}(u)| \geq \frac{|u|}{\alpha} - \frac{Ae^{\sigma R}}{\alpha}. \tag{35}$$

which is true for all $u \in \mathbb{R}$ since $x = g^{-1}(u)$ holds for all real x and u as shown in the first step of the proof. Define the function for all real u

$$\psi(u) = \begin{cases} |u|/\alpha - Ae^{\sigma R}/\alpha & \text{if } |u|/\alpha > Ae^{\sigma R}/\alpha \\ 0 & \text{otherwise} \end{cases} \tag{36}$$

which clearly satisfies $|g^{-1}(u)| \geq |\psi(u)|$. Make $\beta = 1/\alpha$ and multiply both sides of (34) by $1/\alpha$ to see that $|h(w)| = |w/\alpha - g^{-1}(w)|$. Combining these expressions, we can then write for some $A' > 0$ and $w \in g(D_R(x'))$

$$|h(w)| \leq \frac{Ae^{\sigma R}/\alpha}{1 + g^{-1}(u)^2} \leq \frac{Ae^{\sigma R}/\alpha}{1 + \psi(u)^2} \leq \frac{A'}{1 + u^2} \tag{37}$$

As our choice of x' was arbitrary, this is true for any $x' \in \mathbb{R}$ and $|h(u + iv)|$ is of moderate decrease along horizontal lines.

Therefore, the function $h(w)$ is analytic on the strip S_a and it is of moderate decrease on each horizontal line $|\mathrm{Im}(w)| = v$, uniformly in $|v| < a$, as long as $\beta = 1/\alpha$. By the Paley-Wiener theorem [31, Theorem X], we conclude that there exists a constant $C > 0$ such that $|\hat{h}(\xi)| \leq e^{-2\pi b\xi}$ for any $0 \leq b < a$. □

APPENDIX C
PROOF OF THEOREM 3

Construct the function $g(z) = \alpha z + f(z)$ where f is not constant. By Picard's little theorem, there exists at most one value $\alpha > A\sigma$ that $f'(z)$ does not take. For the rest of them, there always exists a $z_o \in \mathbb{C}$ such that $g'(z_o) = \alpha + f'(z_o) = 0$. Then, it is possible to write

$$g(z) - a_0 = (z - z_o)^2[a_2 + a_3(z - z_o) + a_4(z - z_o)^2 + \ldots]. \tag{38}$$

Therefore, the function $g(z) - z_o$ has a zero of order ≥ 2 at z_o. By the Local Mapping Theorem, g is n-to-1 near z_o for $n \geq 2$. Using the argument of analytic continuation of local biholomorphisms in Theorem 2, we conclude that the analytic extensions of h around $g(z_o)$ are multivalued. This excludes the possibility of h being entire, thus, h cannot be bandlimited. If $f(z) = C$ for some $C > 0$, then $h(u) = -C/\alpha$, which is bandlimited in the distributional sense. □

REFERENCES

[1] E. T. Whittaker, "XVIII.—On the functions which are represented by the expansions of the interpolation-theory," *Proceedings of the Royal Society of Edinburgh*, vol. 35, pp. 181–194, 1915.

[2] V. A. Kotelnikov, "On the carrying capacity of the ether and wire in telecommunications," in *Material for the First All-Union Conference on Questions of Communication, Izd. Red. Upr. Svyazi RKKA, Moscow*, 1933.

[3] C. E. Shannon, "Communication in the presence of noise," *Proceedings of the IRE*, vol. 37, no. 1, pp. 10–21, 1949.

[4] F. Bond and C. Cahn, "On sampling the zeros of bandwidth limited signals," *IRE Transactions on Information Theory*, vol. 4, no. 3, pp. 110–113, 1958.

[5] B. F. Logan, "Information in the zero crossings of bandpass signals," *Bell System Technical Journal*, vol. 56, no. 4, pp. 487–510, 1977.

[6] S. Roweis, S. Mahajan, and J. Hopfield, "Signal reconstruction from zero-crossings," August 1998, draft (accessed May 2016) https://www.cs.nyu.edu/ roweis/papers/logan.ps.

[7] S. J. Haavik, "The conversion of the zeros of noise," Master's thesis, University of Rochester, Rochester, NY, 1966.

[8] I. Bar-David, "An implicit sampling theorem for bounded bandlimited functions," *Information and Control*, vol. 24, no. 1, pp. 36–44, 1974.

[9] R. Kumaresan and Y. Wang, "A new real-zero conversion algorithm," in *Proceedings 2000 IEEE International Conference on Acoustics, Speech, and Signal Processing.*, vol. 1, 2000, pp. 313–316 vol.1.

[10] R. J. Duffin and A. C. Schaeffer, "Some properties of functions of exponential type," *Bulletin of the American Mathematical Society*, vol. 44, no. 4, pp. 236–240, 1938.

[11] E. M. Stein and R. Shakarchi, *Complex analysis*, ser. Princeton Lectures in Analysis, II. Princeton University Press, Princeton, NJ, 2003.

[12] J. Selva, "Efficient sampling of band-limited signals from sine wave crossings," *IEEE Trans. Signal Processing*, vol. 60, no. 1, pp. 503–508, 2012.

[13] S. Kay and R. Sudhaker, "A zero crossing-based spectrum analyzer," *IEEE Transactions on Acoustics, Speech and Signal Processing*, vol. 34, no. 1, pp. 96–104, 1986.

[14] T. V. Sreenivas and R. J. Niederjohn, "Zero-crossing based spectral analysis and svd spectral analysis for formant frequency estimation in noise," *IEEE Transactions on Signal Processing*, vol. 40, no. 2, pp. 282–293, 1992.

[15] R. Kumaresan and N. Panchal, "Encoding bandpass signals using zero/level crossings: a model-based approach," *Audio, Speech, and Language Processing, IEEE Transactions on*, vol. 18, no. 1, pp. 17–33, 2010.

[16] S. Mallat, "Zero-crossings of a wavelet transform," *IEEE Transactions on Information Theory*, vol. 37, no. 4, pp. 1019–1033, 1991.

[17] J. W. Mark and T. D. Todd, "A nonuniform sampling approach to data compression," *IEEE Trans. Commun.*, vol. 29, no. 1, pp. 24–32, 1981.

[18] Y. Tsividis, "Continuous-time digital signal processing," *Electron. Lett.*, vol. 39, no. 21, pp. 1551–1552, 2003.

[19] H. Inose, T. Aoki, and K. Watanabe, "Asynchronous delta-modulation system," *Electron. Lett.*, vol. 2, no. 3, pp. 95–96, 1966.

[20] P. Martinez-Nuevo, S. Patil, and Y. Tsividis, "Derivative level-crossing sampling," *IEEE Transactions on Circuits and Systems II: Express Briefs*, vol. 62, no. 1, pp. 11–15, 2015.

[21] Y. Tsividis, "Event-driven data acquisition and continuous-time digital signal processing," in *Custom Integrated Circuits Conference (CICC), 2010 IEEE*, 2010, pp. 1–8.

[22] A. Zakhor and A. Oppenheim, "Reconstruction of two-dimensional signals from level crossings." *Proceedings of the IEEE*, vol. 78, no. 1, pp. 31 – 55, 1990.

[23] S. R. Curtis and A. V. Oppenheim, "Reconstruction of multidimensional signals from zero crossings." *Journal of the Optical Society of America. A, Optics & Image Science*, vol. 4, pp. 221 – 231, 1987.

[24] H. Lai, "Reconstruction methods for level-crossing sampling," Master's Thesis, EECS, MIT, June 2016.

[25] H. J. Landau, "Necessary density conditions for sampling and interpolation of certain entire functions," *Acta Mathematica*, vol. 117, no. 1, pp. 37–52, July 1967.

[26] S. N. Bernstein, *Leçons sur les propriétés extrémales et la meilleure approximation des fonctions analytiques d'une variable réelle*. Paris, 1926.

[27] S. Azizi, D. Cochran, and J. McDonald, "On the preservation of bandlimitedness under non-affine time warping," in *Proc. Int. Workshop on Sampling Theory and Applications*, 1999.

[28] P. Martínez-Nuevo, "Amplitude sampling for signal representation," Ph.D. dissertation, Massachusetts Institute of Technology, 2016.

[29] H. G. Feichtinger and K. Gröchenig, "Theory and practice of irregular sampling," *Wavelets: mathematics and applications*, pp. 305–363, 1994.

[30] S. Banach, "Sur les opérations dans les ensembles abstraits et leur application aux équations intégrales," *Fund. Math*, vol. 3, no. 1, pp. 133–181, 1922.

[31] R. E. A. C. Paley and N. Wiener, *Fourier transforms in the complex domain*. American Mathematical Soc., 1934, vol. 19.

Pablo Martínez-Nuevo received the *Ingeniero de Telecomunicación* degree from the ETSIT, University of Valladolid, Spain, in 2010 and the M.Sc. degree in Electrical Engineering from Columbia University, NY, in 2012 where he was awarded the Edwin Howard Armstrong Memorial Award. He received the Ph.D. degree in Electrical Engineering and Computer Science from the Massachusetts Institute of Technology (MIT) in 2016 under the supervision of Prof. Alan V. Oppenheim in the Digital Signal Processing Group. He has been a recipient of the Fundación Rafael del Pino Fellowship, Madrid, Spain, for graduate studies at MIT.

Dr. Martínez-Nuevo is currently a Sr. Acoustical Researcher at Bang&Olufsen in Denmark. His research interests lie within the areas of signal and information processing, sampling theory, and learning.

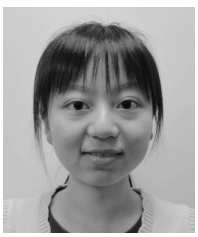

Hsin-Yu Lai received bachelor's degrees in both Electrical Engineering and Mathematics from National Taiwan University in 2014. She received her master's degree in Electrical Engineering and Computer Science (EECS) from the Massachusetts Institute of Technology (MIT) under the supervision of Prof. Alan V. Oppenheim in 2016. During that time, she worked with Dr. Pablo Martínez-Nuevo on amplitude sampling and reconstruction. Hsin-Yu Lai is currently a Ph.D. student in the EECS Department at MIT working with Prof. Vivienne Sze and Prof. Thomas Heldt. Her research interests include signal processing, inference, and algorithm design.

Alan V. Oppenheim (M'65–SM'71–F'77–LF'03) received the S.B. and S.M. degrees in 1961 and the Sc.D. degree in 1964, all in electrical engineering, from the Massachusetts Institute of Technology. He is also the recipient of an honorary doctorate from Tel Aviv University.

In 1964, he joined the faculty at MIT and is currently Professor of Engineering and a MacVicar Fellow. His research interests are in the general area of signal processing, theory, algorithms and its applications. He is coauthor of several widely used textbooks and the editor of several advanced books on signal processing. In Spring 2015, an online version of his Discrete-Time Signal Processing course (6.341) was launched on edX through MIT.

Dr. Oppenheim is a member of the National Academy of Engineering, and a member of Sigma Xi and Eta Kappa Nu. He has been a Guggenheim Fellow and a Sackler Fellow. He has received a number of awards for outstanding research and teaching, including the IEEE Education Medal, the IEEE Jack S. Kilby Signal Processing Medal, the IEEE Centennial Medal and the IEEE Third Millennium Medal. From the IEEE Signal Processing Society he has been honored with the Education Award, the Society Award, the Technical Achievement Award and the Senior Award. He has also received a number of awards at MIT for excellence in teaching, including the Bose Award, the Everett Moore Baker Award, and several awards for outstanding advising and mentoring.